Information geometry theory of bifurcations? A covariant formulation

Cite as: Chaos **32**, 023119 (2022); https://doi.org/10.1063/5.0069033
Submitted: 28 August 2021 • Accepted: 20 January 2022 • Published Online: 16 February 2022

V. B. da Silva, J. P. Vieira and Edson D. Leonel

Information geometry theory of bifurcations? A covariant formulation

Cite as: Chaos **32**, 023119 (2022); doi: 10.1063/5.0069033
Submitted: 28 August 2021 · Accepted: 20 January 2022 ·
Published Online: 16 February 2022

V. B. da Silva,[1,a)] J. P. Vieira,[2] and Edson D. Leonel[1]

AFFILIATIONS

[1]Department of Physics, Universidade Estadual Paulista "Júlio de Mesquita Filho," Campus de Rio Claro, São Paulo 13506-900, Brazil
[2]Department of Mathematics, Universidade Estadual Paulista "Júlio de Mesquita Filho," Campus de Rio Claro, São Paulo 13506-900, Brazil

[a)]**Author to whom correspondence should be addressed:** viniciusx10@yahoo.com.br

ABSTRACT

The conventional local bifurcation theory (CBT) fails to present a complete characterization of the stability and general aspects of complex phenomena. After all, the CBT only explores the behavior of nonlinear dynamical systems in the neighborhood of their fixed points. Thus, this limitation imposes the necessity of non-trivial global techniques and lengthy numerical solutions. In this article, we present an attempt to overcome these problems by including the Fisher information theory in the study of bifurcations. Here, we investigate a Riemannian metrical structure of local and global bifurcations described in the context of dynamical systems. The introduced metric is based on the concept of information distance. We examine five contrasting models in detail: saddle-node, transcritical, supercritical pitchfork, subcritical pitchfork, and homoclinic bifurcations. We found that the metric imposes a curvature scalar R on the parameter space. Also, we discovered that R diverges to infinity while approaching bifurcation points. We demonstrate that the local stability conditions are recovered from the interpretations of the curvature R, while global stability is inferred from the character of the Fisher metric. The results are a clear improvement over those of the conventional theory.

Geometry has been much applied to nonlinear dynamics with particular emphasis on the framework of bifurcations and chaos.[1–3] Nevertheless, previous attempts lack a meaningful metrical structure, that is, the expression for the distance between equilibrium states. In this article, we show that if the information theory is included in the axioms of nonlinear dynamics, then there exists a corresponding Riemannian metric, which allows us to represent dynamical systems by intriguing Riemannian manifolds. The Riemannian metric and the curvature scalar of these manifolds are of exceptional interest because they lead to a new measure of global and local stability of higher order. The interpretation of the Fisher geometry is a new attempt to extract information from complex systems. In addition, information geometry presents a new hope of telling us something new about dynamic systems, particularly, where the standard methods show little or no solution.

I. INTRODUCTION

The main goal of the bifurcation theory is to express sudden qualitative changes in the phase portraits of dynamical systems nearby their local solution branches when control parameters are changed continuously and smoothly.[4,5] Despite the range of applicability, the CBT has, heretofore, been beset by limitations and difficulties. These are due to the fact that the most interesting results of the CBT are only local. As a consequence of that, there is a necessity to employ non-trivial global techniques and time-consuming numerical solutions. In this article, we present an attempt to overcome these problems in the framework of information geometry.

We remark, parenthetically, that bifurcations may be seen as the temporal version of thermodynamic phase transitions, where the asymptotic regime is assumed.[6,7] In other words, one may interpret a phase transition as a bifurcation in the underlying microscopic dynamics.[6]

Recently, many authors have characterized phase transitions in the parameter space of a wide range of classical and quantum systems in the framework of the Fisher information geometry.[8–19] By introducing a Riemannian metrical structure for the parameter space through the definition of the Fisher information metric, one may investigate global and local properties through the study of the Riemannian curvature scalar (R). In this scenario, the curvature R is a distinct quantity in three ways. First, the calculation of R is invariant to thermodynamic coordinates. Second, the divergent behavior of the curvature scalar marks the phenomena of phase transitions in the vicinity of critical points. Third, finally, the concept of stability can be measured by analyzing the metric and the curvature R of the parameter space.

Therefore, the question that is naturally posed here is whether we may apply information geometry to explore critical aspects of bifurcations. More precisely, we inquire whether this geometrical approach may unambiguously extract global and local properties of bifurcations. This article, the first in a series devoted to the above questions, is occupied with the formulation of a meaningful Riemannian metrical structure in the framework of dynamical systems described by differential equations.

Bifurcations refer to a broad range of phenomena in almost all branches of natural sciences, such as chemical reactions,[20–22] electrical circuits,[23–25] biology,[26–28] and others.[29–31] Hence, the application of these new geometrical methods may bring new light to the study of dynamical systems where the CBT has been unsuccessful or incomplete. Based on the above, this article focuses on the generalization of information theory. In this manner, we introduce and investigate a Riemannian metrical structure for local and global bifurcations. Here, the introduced metric is based on Fisher's information distance.[18,32,33] We show here that the geometric bifurcation theory (GBT) correctly predicts the essential critical aspects of the CBT. In addition, the GBT assigns global and local properties of dynamical systems.

This article is organized as follows. In Sec. II, we introduce the formalism of Fisher's information geometry applied to local bifurcations. The third section is concerned with the generalization of information geometry, in which our attention is placed on the study of dynamical systems with homoclinic bifurcations. The fourth section is devoted to the derivation of Fisher's information matrix and curvature R for local bifurcations, in particular, saddle-node, transcritical, and pitchfork. Here, we present physical interpretations of the concept of stability in the structural sense. The fifth section is dedicated to interpreting the curvature R and the Riemannian metric for an example of homoclinic bifurcation. Finally, Sec. VI is devoted to the conclusion of our results and suggestions for further research.

II. THEORY

The general program of this section consists of extending the geometrical methods employed in Fisher's information geometry to investigate bifurcations in the framework of dynamical systems. Therefore, we organize this section as follows. Information theory arises from the investigation of probability density functions[19] (PDF). Thus, we shall first dedicate ourselves to constructing a proper probability distribution to describe nonlinear systems of differential equations. From the knowledge of such probability density, which assigns critical aspects of bifurcations, we describe dynamical systems by the construction of the Riemannian metrical structure of their parameter space. Here, the Riemannian metric and the curvature scalar are of exceptional interest. Third, we interpret the concept of local and global stability in the background of information geometry. Fourth, finally, we generalize our original geometric approach to investigate non-trivial bifurcations in the context of two-dimensional systems.

A. Bifurcation and probability density function

The Fisher information geometry has roots in the study of the manifold of PDFs. The first step to introduce and extend the geometric methods of information theory is the definition of a mathematical model of bifurcations in the framework of dynamical systems. Consequently, the second step will be based on the construction of probability distribution.

The nonlinear differential equation that represents the mathematical model of bifurcations in the context of dynamical systems is given by

$$\beta = \frac{ds}{d\tau} = \Phi\,(s;m)\,, \tag{1}$$

in which β is the momentum, s is the order parameter, τ is the time, and m is the control parameter. In Eq. (1), the normal form $\Phi\,(s;m)$ is a function determined by a potential $U(s;m)$ through the relation $\Phi\,(s;m) = -\partial U\,(s;m)\,/\partial s$. Here, $\Phi(s;m) = 0$ assigns the equilibrium state s^* of the order parameter.[34] A further remark concerns the condition for the appearance of bifurcations. For the model above exhibits bifurcations, we should observe that the eigenvalue Λ of Eq. (1) must be zero at the critical value (s_C^*, m_C). That is,

$$\Lambda = \left(\frac{\partial \Phi(s;m)}{\partial s}\right)_{(s_C^*, m_C)} = 0. \tag{2}$$

This latter addresses the general mathematical condition on the occurrence of bifurcations in the dynamical system.

Furthermore, we should remark here that Eq. (1), which arises from Hamiltonian equations, is unambiguously advantageous since it describes the general form of the dynamical systems in nonlinear sciences.[4,6]

We shall now present the procedure which will be employed for constructing the PDF for the dynamic systems in question. For the continuous system described by Eq. (1), the variable s follows a trajectory through time so that each value of s is only associated with one value of time τ. Following this one-to-one correspondence between the values of s and τ, we may write explicitly[4,6,35]

$$\rho\,(s)\,ds = \rho\,(\tau)\,d\tau, \tag{3}$$

where $\rho\,(s)$ denotes the probability density for observing a particular value of s and $\rho\,(\tau)$ reads the probability of observing a particular time τ. Nevertheless, when sampling along a time interval $[0 - T]$, we shall expressly assume that all times are equally probable. Thus,

Eq. (3) here simplifies to

$$\rho\,(s) = \frac{1}{T\;\Phi\,(s;m)}, \tag{4}$$

in virtue of Eq. (1).

The latter equation teaches us that the probability density to observe a particular value of s is inversely proportional to the normal form of the dynamical systems of Eq. (1). This formulation is not a new idea here. In fact, it is present in the recent developments of the Fisher information to study sustainable and ecological systems.[35] Based on the correspondence principle, Eq. (3), the PDF formulation presented right above yields a peculiar expression for the probability in the framework of dynamical systems.

On the other hand, we note that Eq. (4) diverges at the equilibrium state of $\Phi(s;m)$. Therefore, we may conclude that the existence of such divergence serves to emphasize that the present PDF must, in some respect, be incomplete. Based on the above, we now seek a formulation that enables us to retain the evident correspondence principle and offers something akin to the advantage of the mathematical model of bifurcations defined above.

The desired formulation is to be found in that between the moment β of the dynamical system and its normal form $\Phi\,(s;m)$ by writing the probability density $\rho(\beta)$ of the variable β from the knowledge of the probability $\rho(s)$ of s. To exploit this alternative, a transformation of variables is necessary to enable us to determine $\rho(\beta)$. We shall perform this transformation with the aid of the Fourier integral representation of characteristic functions.[36–38]

In order to alter Eq. (4) in the above-outlined manner, let $g(\kappa)$ be the characteristic function of the variable β. If $\beta = \Phi(s;m)$, then we write

$$g(\kappa) = \left\{\exp\left(J\kappa\;\beta\right)\right\} = \left\{\exp\left(J\kappa\;\Phi\,(s;m)\right)\right\}$$

or simply

$$g(\kappa) = \int ds\, e^{J\kappa\;\Phi(s;m)}\rho\,(s)\,, \tag{5}$$

where J denotes the imaginary unity $\sqrt{-1}$.

Nevertheless,

$$\rho\,(\beta) = \frac{1}{2\pi}\int d\kappa\; e^{-J\kappa\;\beta}g\,(\kappa)\,, \tag{6}$$

whence we obtain[39]

$$\rho\,(\beta) = \frac{1}{2\pi}\int\int ds\,d\kappa\,\exp\left[-J\kappa\;\left(\beta - \Phi(s;m)\right)\right]\rho\,(s)\,. \tag{7}$$

On recalling the integral representation of Dirac delta distribution,

$$\delta\,(s) = \frac{1}{2\pi}\int d\kappa\,\exp\left(-J\kappa\;s\right), \tag{8}$$

we arrive at

$$\rho\,(\beta) = \int ds\,\delta\,(\beta - \Phi(s;m))\,\rho\,(s)\,. \tag{9}$$

An alternative representation is obtained by writing

$$\rho\,(\beta) = \frac{1}{T}\int_0^T \rho\,(\tau)\,d\tau\,\delta\,(\beta - \Phi(s;m))\,, \tag{10}$$

in virtue of Eq. (3). However, the right-hand side of the integrand is independent of τ. Thus, the solution to Eq. (10) has the form

$$\rho(\beta) = \delta\,(\beta - \Phi(s;m))\,, \tag{11}$$

which may be reduced in the following well-known Gaussian representation[38,40]

$$\rho\,(\beta) = \delta_T\,(\beta - \Phi(s;m)) = \sqrt{\frac{T}{\pi}}\exp\left[-\left(\beta - \Phi(s;m)\right)^2 T\right]. \tag{12}$$

We must recognize that the latter equation is only consistent when T is large. Nevertheless, to make Eq. (12) mathematically and physically meaningful without significantly altering thereby the physical properties represented in the above formulation, we must address further considerations on how large T must be in the context of dynamical systems and bifurcations.

It is well-known that bifurcations may be interpreted as the temporal version of phase transitions.[6,7] Nevertheless, we must bring to our attention that phase transitions are only well-defined in the thermodynamic limit. In this limit, the system's extensive parameters, for example, the volume (V) and the number of particles (N), are allowed to increase without bound such that the intensive ratios, e.g., N/V, remain finite.[41]

Hence, one can conclude that T here should be infinitely large so that we may interpret bifurcations as the temporal version of phase transitions. Indeed, one must understand T as a limiting case to what one expects to be a correct approximation for the solutions of Eq. (1) at long but finite times. In this manner, we infer that Eq. (12) is valid when T acts as a limit that must be as large as we like. As a consequence of that, we may keep the dominant terms of Eq. (12) and draw out the relevant concepts of bifurcations. This is similar to the context of statistical mechanics, in which the thermodynamic limit is crucial for physical systems to exhibit clear-cut phase transitions.[6,41]

The derivation of the probability density $\rho(\beta)$ proves the correctness of the considered choice of transformation of variables, Eq. (5), because we have obtained a compelling PDF that removes the divergent character of Eq. (4) and assigns critical aspects of the bifurcations given by Eq. (1). Based on the above, we now proceed to the construction of information geometry in the framework of dynamical systems.

B. Information geometry

To introduce the Fisher Riemannian metrical structure into the space of parameters of dynamical systems, let us consider Ω a family of probability distributions that is smoothly parametrized by two real parameters,[18,32,33] in which

$$\Omega = \left\{\mathcal{P}_X = \frac{\rho(\beta;X)}{T};\, T\in\mathbb{R}^+;\, X\in\mathbb{R}^2, X = \left(X^1, X^2\right)\right\}. \tag{13}$$

The statistical model Ω of random variable β carries the structure of a smooth Riemannian manifold $\mathcal{M}$ with respect to which $X = \left(X^1, X^2\right) = (s,m)$ play the role of coordinates of a point $\mathcal{P}_X \in \Omega$. Here, the model's metric is defined by the Fisher matrix $\mathrm{H} = (\mathbf{G}_{\alpha\mu}(\mathbf{X}))$. The components of the metric tensor are calculated as the expectation of a product that involves partial derivatives of the

PDF of Eq. (12). That is,

$$G_{11}(X) = \langle (\mathrm{W}^1)^2 \rangle = \int_{-\infty}^{+\infty} d\beta \left[\frac{\partial^2}{\partial s^2} \left(\frac{-\ln \rho(\beta)}{T} \right) \right] \rho(\beta), \quad (14)$$

$$G_{22}(X) = \langle (\mathrm{W}^2)^2 \rangle = \int_{-\infty}^{+\infty} d\beta \left[\frac{\partial^2}{\partial m^2} \left(\frac{-\ln \rho(\beta)}{T} \right) \right] \rho(\beta), \quad (15)$$

where the statistical quantities $\mathrm{W}^\mu = \partial \ln \rho / \partial X^\mu$ form a basis of a vector space of random variable β, which is identified with the tangent space $\eta_X \Omega$. Consequently, we can define the operator of covariant differentiation and some of the different connections using the one-to-one correspondence between Ω and Riemannian manifold.

On account of the fact that the probability to measure W^1 does not necessarily affect W^2 and both have equal probability to be observed, we may then write[18,32,33,41]

$$G_{21}(X) = \langle \mathrm{W}^1 \mathrm{W}^2 \rangle = \int_{-\infty}^{+\infty} d\beta \left[\frac{\partial \ln \rho(\beta)}{\partial s} \frac{\partial \ln \rho(\beta)}{\partial m} \right] \frac{\rho(\beta)}{T}, \quad (16)$$

which describes the off-diagonal components of the Fisher information matrix.

An alternative representation, the one we shall consider for the calculations henceforth, is obtained by substituting Eq. (12) into Eqs. (14)–(16), in which we obtain

$$G_{11} = \langle (\mathrm{W}^1)^2 \rangle = \lim_{T \to \infty} \int_{-\infty}^{+\infty} d\beta \, A(\beta) \delta_T (\beta - \Phi(s;m)), \quad (17)$$

where

$$A(\beta) = \frac{1}{T} \left[\frac{\partial^2}{\partial s^2} \left(-\ln \left[\delta_T (\beta - \Phi(s;m)) \right] \right) \right], \quad (18)$$

$$G_{22} = \langle (\mathrm{W}^2)^2 \rangle = \lim_{T \to \infty} \int_{-\infty}^{+\infty} d\beta \, B(\beta) \delta_T (\beta - \Phi(s;m)), \quad (19)$$

where

$$B(\beta) = \frac{1}{T} \left[\frac{\partial^2}{\partial m^2} \left(-\ln \left[\delta_T (\beta - \Phi(s;m)) \right] \right) \right] \quad (20)$$

and

$$G_{21} = \langle \mathrm{W}^1 \mathrm{W}^2 \rangle = \lim_{T \to \infty} \int_{-\infty}^{+\infty} d\beta \, C(\beta) \delta_T (\beta - \Phi(s;m)), \quad (21)$$

where

$$C(\beta) = \frac{1}{T} \left[\frac{\partial \ln \left[\delta_T (\beta - \Phi(s;m)) \right]}{\partial s} \frac{\partial \ln \left[\delta_T (\beta - \Phi(s;m)) \right]}{\partial m} \right]. \quad (22)$$

Nevertheless, we may, in virtue of the well-known properties of Dirac delta distribution, simply write[42]

$$G_{11} = \lim_{T \to \infty} \sqrt{\frac{T}{\pi}} \int_{-\infty}^{+\infty} d\beta \, \tilde{A}(\beta) \mathrm{e}^{-(\beta - \Phi(s;m))^2 T}, \quad (23)$$

where

$$\tilde{A}(\beta) = \left[2 \left(\frac{\partial \Phi}{\partial s} \right)^2 - 2 (\beta - \Phi) \left(\frac{\partial^2 \Phi}{\partial s^2} \right) \right]. \quad (24)$$

It can also be shown, analogous to Eq. (23), that

$$G_{22} = \lim_{T \to \infty} \sqrt{\frac{T}{\pi}} \int_{-\infty}^{+\infty} d\beta \, \tilde{B}(\beta) \mathrm{e}^{-(\beta - \Phi(s;m))^2 T}, \quad (25)$$

where

$$\tilde{B}(\beta) = \left[2 \left(\frac{\partial \Phi}{\partial m} \right)^2 - 2 (\beta - \Phi) \left(\frac{\partial^2 \Phi}{\partial m^2} \right) \right]. \quad (26)$$

For the off-diagonal components, we have

$$G_{21} = G_{12} = \lim_{T \to \infty} \sqrt{\frac{T}{\pi}} \int_{-\infty}^{+\infty} d\beta \, \tilde{C}(\beta) \mathrm{e}^{-(\beta - \Phi(s;m))^2 T}, \quad (27)$$

in which

$$\tilde{C}(\beta) = \left[4T \left(\frac{\partial \Phi}{\partial s} \right) \left(\frac{\partial \Phi}{\partial m} \right) (\beta - \Phi)^2 \right]. \quad (28)$$

On recalling that[38,42]

$$\lim_{T \to \infty} \sqrt{\frac{T}{\pi}} \int_{-\infty}^{+\infty} d\beta \, \psi(\beta) \exp \left[-(\beta - \Phi(s;m))^2 T \right] = \psi(\Phi), \quad (29)$$

the solutions to Eqs. (23)–(25) have the form

$$G_{11} = 2 \left(\frac{\partial \Phi(s;m)}{\partial s} \right)^2, \quad (30)$$

$$G_{22} = 2 \left(\frac{\partial \Phi(s;m)}{\partial m} \right)^2, \quad (31)$$

and

$$G_{21} = G_{12} = 0. \quad (32)$$

Consequently, the Fisher information matrix H is given by

$$\mathrm{H} = \begin{bmatrix} 2 \left(\frac{\partial \Phi(s;m)}{\partial s} \right)^2 & 0 \\ 0 & 2 \left(\frac{\partial \Phi(s;m)}{\partial m} \right)^2 \end{bmatrix}. \quad (33)$$

We note, incidentally, that W^1 and W^2 are statistically independent. As a consequence of that, we then have the expectation or the average value of $\langle \mathrm{W}^1 \mathrm{W}^2 \rangle$ equal to the product of their mean values,[36,37,41] that is, $\langle \mathrm{W}^1 \rangle \langle \mathrm{W}^2 \rangle$. Since each of these is zero, so is $G_{21} = G_{12}$.

We may conclude, without further calculation, that the Fisher matrix $\mathrm{H} = G_{\alpha\mu}(X)$ is positive definite because it is a diagonal square matrix of the squared first-order derivatives of the normal form $\Phi(s;m)$, which show themselves independent of β. Finally, we should remark that the matrix H led us to the well-known geometrically invariant second fundamental form,[32,43]

$$d\ell^2 = G_{11}(ds)^2 + G_{22}(dm)^2, \quad (34)$$

in which $d\ell$ denotes the local quadratic distance in the parameter space. With our aim of deriving local statements in mind, we define the metric in respect to the reference fixed-point s^*. Therefore, we must recognize that the metric elements $G_{\alpha\mu}$ are evaluated in the state $s = s^*$. Defining Riemannian metrics in the neighborhood of a

reference state is not a new idea here. This has already been discussed in other contexts.[44,45] From the derivation of the Fisher metric, which describes a proper distance in the parameter space of dynamical systems, we shall now proceed to the calculation of the Riemannian curvature scalar.

The curvature R is a natural consequence and an immediate application of the Fisher geometry above, given the fact that it reveals intrinsic properties of physical systems, especially in the neighborhood of the critical points. In addition, we should note that the calculation of R is invariant to thermodynamic coordinates, and the divergent behavior of the curvature scalar is rigorously related to the well-known phenomena of phase transitions.

The metric Eq. (34) induces a curvature R on the manifold of the parameter space X,[46]

$$\mathrm{R} = \frac{1}{\sqrt{G}}\left[\frac{\partial}{\partial s}\left(\frac{1}{\sqrt{G}}\frac{\partial G_{22}}{\partial s}\right) + \frac{\partial}{\partial m}\left(\frac{1}{\sqrt{G}}\frac{\partial G_{11}}{\partial m}\right)\right], \tag{35}$$

in which $G \equiv G_{11}G_{22}$. Originally, the expression of the curvature scalar presents a negative sign. Here, we, henceforth, confine ourselves to the standard Weinberg sign convention,[13,47] in which the negative sign of R is suppressed.

In order to consider R as a new quantity to investigate dynamical systems, we must, therefore, interpret it accordingly to our statistical approach. Furthermore, we must investigate the conditions for the occurrence of bifurcations in Eq. (35).

We recognize that the curvature R presented right above is connected to our statistical formulation since, statistically, we can conclude that R is a function of the second and the third moments of the variables W^{α}. Physically, we recognize that R is inversely proportional to the first-order derivatives of $\Phi(s;m)$. In general, however, $\partial\Phi(s;m)/\partial m$ contributes with a non-zero constant. Hence, we may see from Eq. (35) that

$$\mathrm{R} \to \pm\infty \quad \text{as} \quad \left(\frac{\partial\Phi}{\partial s}\right) \to 0, \tag{36}$$

which directly implies the remarkable condition for the occurrence of bifurcations, Eq. (2), when the metric coefficients are evaluated at the critical value $(s_{\mathrm{C}}^{*}, m_{\mathrm{C}})$. Thus, we predict that R should diverge at the singularities of dynamical systems, which appear at the bifurcation points, i.e., at critical values of the equilibrium state s^{*}.

In the investigation of physical systems in the framework of information geometry, we must also recognize that the divergent behavior of R marks the phenomena of phase transitions at critical points.[8–12,16,17] Therefore, our formulation is in good agreement with the standpoint of information geometry as we may conclude that the divergence of R implies the phenomena of bifurcations nearby the singularities of dynamical systems, just like the divergence of R refers to phase transitions in statistical mechanics.

To conclude, we have obtained a new intriguing possibility to investigate and describe dynamical systems, particularly in the neighborhood of bifurcation points, through the calculation of the Fisher metric and curvature R.

C. The sign of R

Stability is an additional crucial concept in the understanding of physical systems. In the present section, we investigate the concepts of local and global stabilities in the framework of the recent developments of information geometry based on the interpretation of the Riemannian metric and the curvature scalar's sign.[8–12,16–19]

In actuality, the behavior of the second-order derivatives of thermodynamic potentials reads the local stability criteria of a given physical system in statistical mechanics. More specifically, if a thermodynamic potential is a convex function of its extensive variables and a concave function of its intensive variables, we may then conclude that the physical system is stable.[48]

In the framework of information geometry, however, Janyszek and Mrugała found that the curvature R is a function of the second and third derivatives of thermodynamic potentials. Furthermore, R diverges at critical points. As a consequence of these facts, R may also be interpreted as a higher-order measure of stability.[16]

Previous studies revealed important conclusions about the interpretation of the sign of R on stability.[16,17,49] In the study of quantum gases, for example, the sign of the curvature scalar is uniformly negative for the Bose gas. In addition, the curvature R decreases from zero to negative infinity in the condensation region, thus indicating that bosons are less stable.[50] Nevertheless, the sign of the curvature R for the Fermi gas revealed to be uniformly positive. This indicates that fermions are more stable than bosons. The conclusions that regard the signs of R, surprisingly, are in agreement with the Pauli principle.[16,17,49] In the light of the foregoing, we may write that stable systems have positive R, while unstable systems must exhibit negative R.

However, we must recognize that R is a quantity that describes the local stability of thermodynamic systems because the computation of the curvature reveals whether a phase is in local maximum or minimum in the neighborhood of critical points, given the fact that R may be uniformly positive or negative depending on values of the parameters.[9,10] Hence, a necessary and sufficient condition to ensure the global thermodynamic stability, following probability considerations, is determined by verifying the well-known requirements of the Sylvester criterion,[9,10,12–15,51] in which

$$\begin{aligned} \Delta_1 &= G_{11} > 0, \\ \Delta_2 &= \begin{vmatrix} G_{11} & G_{12} \\ G_{21} & G_{22} \end{vmatrix} > 0, \\ \Delta_3 &= \begin{vmatrix} G_{11} & G_{12} & G_{13} \\ G_{21} & G_{22} & G_{23} \\ G_{31} & G_{23} & G_{33} \end{vmatrix} > 0. \end{aligned} \tag{37}$$

If all the principal minors of the metric tensor are positive definite, that is to say, the determinants $\Delta_i > 0$, then the thermodynamic metric elements $G_{\alpha\mu}$ constitute a positive definite matrix. Hence, we may conclude that the system is globally stable, regardless of the sign of R. Finally, we note that Δ_3 is neglected in two-dimensional geometries.

Based on the above, the question naturally posed is whether such notions of stability could be extended for our geometric formulation of dynamical systems.

In order to describe the interpretation of stability for our approach from the standpoint of Riemannian geometry, we examine the relationship between the stability criteria of dynamical systems and the result expressed by Eq. (36) that relates the curvature R derived above.

In general, there are different definitions of stability in nonlinear sciences.[52–57] Considering the purposes of the present paper, for simplicity, we may restrict ourselves to the stability of equilibrium states and the structural stability, that is, the stability of dynamical systems described by differential equations.

The stability of an equilibrium relies on the study of the behavior of the equilibrium solutions to differential equations due to a perturbation of their initial conditions.[52,53] This comprehension of stability may also be understood from the viewpoint of the CBT. More precisely, the stability interpretation of an equilibrium state is given by the analysis of the sign of the second derivatives of the potential $U(s;m)$ or the first derivatives of the normal form $\Phi(s;m)$ nearby the critical equilibrium states of autonomous dynamical systems.[4,7]

We should remark that, in principle, for a stable critical equilibrium state, one may address stability considerations for the system under study, i.e., we may write that a dynamical system is stable if one could prove the existence of the well-known Lyapunov functions.[52,58] The theoretical formulation of these functions is essentially based on a generalization of the idea of the total energy of a given physical system. Nevertheless, the construction of these functions is not usually a simple task. In fact, the lack of robust methods for generating Lyapunov functions imposes several difficulties and practical problems on the study of the stability of dynamic systems through this method.[31,52]

On the other hand, structural stability is associated with the conservation of the topology of the phase portraits when the system's differential equations are perturbed through the variation of control parameters.[52–57] In other words, a system is structurally stable if the resulting flow is topologically equivalent to the initial one for a sufficiently small perturbation of the control parameters of the differential equations that describe this system.

In addition, it should be remarked, parenthetically, that we may also understand structural stability in a local sense. According to Hazewinkel,[54] one may define the concept of local structural stability as the preservation of all topological properties of the system in some neighborhood of an equilibrium state, s^*, of a continuous-time dynamical system under any sufficiently small perturbation of the system. That is to say, local structural stability denotes a property not of the equilibrium s^* itself but of the system considered in a neighborhood of the state s^*.

Having introduced the different notions of stability, we shall now present the relation between the concepts of bifurcations, structural stability, and the curvature scalar. Based on the above, if one varies the control parameter of the system, for example, m, nearby a critical value, m_C, thereby imposing a qualitative change in the phase portrait, then we may write that the system is no longer structurally stable but structurally unstable. More precisely, we may write that this topological change is called bifurcation. Furthermore, the bifurcation point (s_C^*, m_C) is the one in which the qualitative modification of the phase portrait takes place and leads to the loss of system's structural stability.

Thus, we conclude that bifurcations are, of course, intimately tied to the concept of structural stability of dynamical systems. Based on the above, let us now return to the result expressed by Eq. (36), which directly implies the remarkable condition for the occurrence of bifurcations.

As we have demonstrated, Eq. (36) basically teaches us that the curvature R should diverge at the singularities of dynamical systems. These singularities appear at the bifurcation points. On account of the interpretation of Eq. (36) and the stability definitions presented above, we may write that if the curvature R diverges at the bifurcation point of dynamical systems and bifurcations are tied to the loss of the structural stability of a system, then we can conclude that the curvature may be interpreted as a new higher-order measure of stability of dynamical systems.

Nevertheless, in the framework of Riemannian geometry,[16,45] we must recognize that the curvature scalar is a local measure of stability since the computation of the curvature R only reveals whether a phase is in local maximum or minimum in the neighborhood of critical points of physical systems, given the fact that R may be uniformly positive or negative depending on values of the control parameters.

Hence, in analogy with the interpretation of R in the framework of Riemannian geometry[16,45] along with the concept of local structural stability,[54] we understand that the curvature scalar is a measure of the local structural stability of dynamical systems because the curvature R reveals itself as a measure of the stability properties of a dynamical system in the vicinity of the critical values of equilibrium states.[52,54] Furthermore, we may expect a positive curvature R for local structural stable systems. On the other hand, locally structural unstable systems must exhibit negative R.

Nonetheless, we must emphasize that R is a local measure of stability. Therefore, with the aim of determining global statements in mind, we shall now turn to the interpretation of global stability in the framework of Riemannian geometry.

In analogy with the treatment of statistical mechanics, one may see that Eqs. (30)–(33) satisfy the necessary and sufficient conditions of the Sylvester criterion, Eq. (37). Consequently, we may write that the dynamical systems described by the differential equation Eq. (1) are globally stable, regardless of the possible signs of R.

However, we must remark, further, that this global stability through the viewpoint of the Sylvester criterion should be interpreted in the sense of the structural stability of the system, that is, the stability as a whole, because the violation of the Sylvester criterion is a necessary condition for the dynamical system, Eq. (1), reaches the bifurcation point, and becomes structurally unstable.[52,55–57] Alternatively, we may then write that the verification of the conditions of the Sylvester criterion is necessary for a dynamical system to exhibit structural stability.

To conclude, we have, so far, developed and extended many features of the Fisher information geometry to investigate bifurcations of dynamical systems expressed by differential equations. As a result, we have obtained an intriguing quantity named Ricci curvature scalar, henceforth denoted by R, which reveals itself as a function of the derivatives of Φ.

From the standpoint of Riemannian geometry, we have also obtained new interpretations of the concept of stability. In particular, we have concluded that the curvature R presents itself as a new

local measure of the structural stability for the dynamical systems in the framework of differential equations. Consequently, we may predict that the curvature should be positive for locally structural stable systems. Finally, it should be remarked that the positive defined metric of the dynamical system, Eq. (1), satisfies the sufficient and necessary conditions to ensure global stability in the structural sense.

III. GENERALIZATION TO TWO-DIMENSIONAL SYSTEMS

The entire development of the above sections remained restricted to the realm of bifurcations in the framework of dynamical systems of a single differential equation. Such consideration is not a restriction but, rather, can be extended at will. In the present article, however, we also aim at dynamic systems in two dimensions, while the proper application of our geometric methods to the N-dimensional case will be postponed to the second article of this series, in which limit cycles and Hopf bifurcations will be investigated in details.

The program of the generalization to be presented relies on the construction of the Riemannian metrical structure of the parameter space of two-dimensional systems. Our attention here is to apply the geometric methods of information geometry to investigate homoclinic bifurcations.

Therefore, we organize this section as follows. We shall first present a revised account of the developments in Sec. II regarding the derivation of the probability density function of one-dimensional systems. Second, we extend the original formulation for a system of differential equations. Finally, we dedicate ourselves to the derivation of the Fisher metric and the curvature R.

According to Sec. II A, the nonlinear differential equation that represents the mathematical model of bifurcations in one spatial dimension, Eq. (1), leads us to a Gaussian PDF with the aid of the Fourier characteristic functions.

In order to generalize Eq. (12), we must extend the original mathematical model of bifurcations. The model for a two-dimensional dynamical system is given by

$$\begin{cases} \beta_1 = \dfrac{ds_1}{d\tau} = \Phi_1(s_1, s_2), \\ \beta_2 = \dfrac{ds_2}{d\tau} = \Phi_2(s_1, s_2). \end{cases} \tag{38}$$

In the present bifurcation model, we employ the following notation: β_1 and β_2 are the momenta. The order parameters are s_1 and s_1. τ is the time. Φ_1 and Φ_2 are non-linear functions, in which it is understood that both may show dependence on one or more varying control parameters. Finally, we note that $\Phi_1 = \Phi_2 = 0$ assigns the equilibrium states (s_1^*, s_2^*) of the order parameters. Furthermore, we should remark that the present two-dimensional mathematical model of bifurcations, Eq. (38), is advantageous as it also describes the general form of the two-dimensional systems in non-linear dynamics.[4,6]

For the model of bifurcations outlined above, the Dirac delta probability function in two dimensions is now realized by

$$\rho(\beta_1, \beta_2) = \delta(\beta_1 - \Phi_1(s_1, s_2),\ \beta_2 - \Phi_2(s_1, s_2)) \tag{39}$$

or simply

$$\rho(\beta_1, \beta_2) = \delta_T(\beta_1 - \Phi_1(s_1, s_2))\, \delta_T(\beta_2 - \Phi_2(s_1, s_2)), \tag{40}$$

which may also be reduced in the following well-known Gaussian representation,[59–61]

$$\rho(\beta_1, \beta_2) = \left(\frac{T}{\pi}\right) e^{-T\left[(\beta_1-\Phi_1)^2+(\beta_2-\Phi_2)^2\right]}. \tag{41}$$

The probability density of Eq. (40) follows the same procedure used in the derivation of Eq. (12).

One should observe that the latter equation is consistent only when $T \to \infty$. In agreement with the developments contained in Sec. II, for bifurcations may be seen as the temporal version of phase transitions in two-dimensional systems, we must understand T as a limiting case to what is expected to be a correct approximation to the solutions to Eq. (38) at long but finite times. Based on the above, we now proceed to the construction of the Riemannian metric and curvature scalar.

To introduce the Riemannian metrical structure into the space of parameters of two-dimensional systems, Eq. (38), let us consider Ω as a family of probability distributions. Here, Ω is smoothly parametrized by three real parameters,[62] in which

$$\Omega = \left\{ \mathcal{P}_X = \frac{\rho(\beta_1, \beta_2; X)}{T};\ T \in \mathbb{R}^+;\ X \in \mathbb{R}^3 \right\}, \tag{42}$$

where the statistical model Ω carries the structure of a Riemannian manifold $\mathcal{M}$ of variables β_1 and β_2. In this model, $X = \left(X^1, X^2, X^3\right) = (s_1, s_2, m)$ plays the role of coordinates of a point $\mathcal{P}_X \in \Omega$. Here, the metric is defined by the Fisher matrix $\mathrm{H} = (\mathbf{G}_{\alpha\mu}(\mathbf{X}))$.

Following the procedure used in the derivation of the components of the metric tensor $G_{\alpha\mu}$ for one-dimensional systems, presented in Sec. II B, we find that

$$G_{\alpha\alpha} = \left(\frac{T}{\pi}\right) \int_{-\infty}^{+\infty} \int_{-\infty}^{+\infty} d\beta_1 d\beta_2\, A_\alpha e^{-T\left[(\beta_1-\Phi_1)^2+(\beta_2-\Phi_2)^2\right]}, \tag{43}$$

where

$$A_\alpha = A_\alpha(\beta_1, \beta_2) = \left[2\left(\frac{\partial \Phi_1}{\partial X^\alpha}\right)^2 - 2(\beta_1 - \Phi_1)\left(\frac{\partial^2 \Phi_1}{\partial (X^\alpha)^2}\right) + 2\left(\frac{\partial \Phi_2}{\partial X^\alpha}\right)^2 - 2(\beta_2 - \Phi_2)\left(\frac{\partial^2 \Phi_2}{\partial (X^\alpha)^2}\right) \right].$$

For the off-diagonal components, we have

$$G_{\alpha\mu} = \int_{-\infty}^{+\infty} \int_{-\infty}^{+\infty} d\beta_1 d\beta_2\, B_{\alpha\mu} e^{-T\left[(\beta_1-\Phi_1)^2+(\beta_2-\Phi_2)^2\right]}, \tag{44}$$

whence

$$B_{\alpha\mu} = B_{\alpha\mu}(\beta_1, \beta_2) = \frac{4T^2}{\pi}\left[(\beta_1 - \Phi_1)^2 \left(\frac{\partial \Phi_1}{\partial X^\alpha}\right)\left(\frac{\partial \Phi_1}{X^\mu}\right) + (\beta_2 - \Phi_2)^2 \left(\frac{\partial \Phi_2}{\partial X^\alpha}\right)\left(\frac{\partial \Phi_2}{\partial X^\mu}\right) + (\beta_1 - \Phi_1)(\beta_2 - \Phi_2) \times \left(\left(\frac{\partial \Phi_1}{\partial \mathbf{X}^\alpha}\right)\left(\frac{\partial \Phi_2}{\partial \mathbf{X}^\mu}\right) + \left(\frac{\partial \Phi_1}{\partial \mathbf{X}^\mu}\right)\left(\frac{\partial \Phi_2}{\partial \mathbf{X}^\alpha}\right) \right) \right].$$

In Eqs. (43) and (44), both indices α and μ range over the integers 1, 2, and 3, where $\alpha \neq \mu$. Here, $X^1 = s_1$, $X^2 = s_2$, and $X^3 = m$. We must remark that the limit $T \to \infty$ is understood in Eqs. (43) and (44).

On recalling that[60,61]

$$\left(\frac{T}{\pi}\right)\int_{-\infty}^{+\infty}\int_{-\infty}^{+\infty} d\beta_1 d\beta_2\, \psi(\beta_1,\beta_2) e^{-T\left[(\beta_1-\Phi_1)^2+(\beta_2-\Phi_2)^2\right]} = \psi(\Phi_1,\Phi_2),$$

in which the limit $T \to \infty$ is understood, the solutions to Eqs. (43) and (44) have the form

$$G_{\alpha\alpha} = 2\left[\left(\frac{\partial\Phi_1}{\partial X^\alpha}\right)^2 + \left(\frac{\partial\Phi_2}{\partial X^\alpha}\right)^2\right], \tag{45}$$

$$G_{\alpha\mu} = G_{\mu\alpha} = 0. \tag{46}$$

Thus, we may conclude, without further calculation, that two-dimensional systems have a positive definite Fisher matrix $\mathrm{H} = G_{\alpha\mu}(X)$, given the fact that it is a diagonal square matrix, in which the components are the squared first-order derivatives of the normal forms Φ_i. Furthermore, one can readily see that metric elements show themselves independent of β_1 and β_2.

We must observe, finally, that the matrix H yields the following second fundamental form:[32,43]

$$d\ell^2 = G_{11}(ds_1)^2 + G_{22}(ds_2)^2 + G_{33}(dm^2), \tag{47}$$

whence $d\ell$ denotes the local quadratic distance in the parameter space. With our aim of investigating global bifurcations in mind, we cannot define this metric in the neighborhood of a reference state. Otherwise, the Riemannian metric would lead us into a null curvature R. This retrieves no information about the dynamical system under study.[63]

From the derivation of the Fisher metric, which describes a proper distance in the parameter space of dynamical systems, we shall now proceed to the calculation of the Riemannian curvature scalar.

The metric of Eq. (47) induces a curvature R on the manifold of the parameter space X. The challenge now is to carry out the derivation of the curvature R for three-dimensional geometries. In higher dimensions, we must note, however, that the curvature is no longer expressed by Eq. (35). Consequently, the general program to write the curvature scalar is the computation of the Christoffel symbols and then the fourth-rank curvature tensor. Thus, we shall calculate R as follows.[43]

First, one needs to obtain the Christoffel symbols. That is,

$$\Gamma^\alpha_{\xi\sigma} = \frac{1}{2}G^{\mu\alpha}\left(G_{\mu\xi,\sigma} + G_{\mu\sigma,\xi} - G_{\xi\sigma,\mu}\right), \tag{48}$$

in which the comma notation denotes partial differentiation to the parameters s_1, s_2, and m.

Based on the above, we calculate the curvature tensor by employing

$$\mathrm{R}^\alpha_{\xi\sigma l} = \Gamma^\alpha_{\xi\sigma,l} - \Gamma^\alpha_{\xi l,\sigma} + \Gamma^\mu_{\xi\sigma}\Gamma^\alpha_{\mu l} - \Gamma^\mu_{\xi l}\Gamma^\alpha_{\mu\sigma}. \tag{49}$$

Finally, the Riemannian curvature scalar is

$$\mathrm{R} = G^{\mu\nu}\mathrm{R}^\vartheta_{\mu\vartheta\nu}. \tag{50}$$

We may observe that the derivation of curvature R in the parameter space of two-dimensional dynamic systems involves nontrivial algebraic computations because the parameter space is a tridimensional geometry.[64]

To conclude, we have extended the Fisher information geometry to investigate bifurcations of two-dimensional systems expressed by differential equations. The present generalization is in agreement with the standpoint of the Fisher information on higher geometries.[9,14,15]

In Sec. IV, we shall apply and illustrate our proper formulation derived here to study the curvature R and the Riemannian metric for a few examples of bifurcations.

IV. RESULTS I

In this section, we shall apply the results of our method to study the behavior, stability conditions, curvature R, and the character of the transitions of four contrasting cases of local bifurcations, according to the theory developed in Sec. II. The procedure that will be employed in Secs. IV A–IV C is analogous to that considered by Janyszek to investigate magnetic models.[16,17] Thus, we may organize this section as follows. First, we introduce the bifurcation model and its respective normal form.

Second, we aim at stability conditions. Therefore, we first obtain the Fisher metric tensor by computing the derivatives of Φ. As discussed earlier, it should be remarked that the Riemannian metric is defined with respect to the reference state s^*. Therefore, we must recognize that the metric elements $G_{\alpha\mu}$ are evaluated in the state $s = s^*$.

Third, global stability is analyzed according to the Sylvester criterion. Our task here is to interpret the local square distance ($d\ell^2$) to verify whether or not the determinants Δ_i are positive definite. Then, we dedicate ourselves to the local structural stability analysis. In this latter, we first evaluate the components of the metric tensor at the equilibrium state of the order parameter. Then, we compute and interpret the curvature scalar nearby the bifurcation point. Here, we emphasize that the analysis of curvature scalar and the Sylvester criterion defines the structural stability criteria of a dynamical system in the framework of Riemannian geometry.

Finally, we interpret the diagrams of the curvature R with interest in the character of its divergence. We must note that the divergence of R may reveal different transitions.[65,66] The first type of transition is evident when the singularities of the curvature R coincide with the singularities of dynamical systems. These singularities appear at the bifurcation points. Such behavior denotes a transition of type I, which may be seen as a second-order transition in respect to the Ehrenfest classification scheme.[41,67]

On the other hand, if the curvature R changes its sign and diverges in the neighborhood of the bifurcation point, then one has

a transition of type II, which may be interpreted as a first-order transition in the context of the Ehrenfest classification.

A. Saddle-node bifurcation

The saddle-node bifurcation describes a mechanism for the disappearance or appearance of equilibrium states.[5,7,68] In general, smooth transitions are governed by saddle-node bifurcations, whose presence is remarkable in the study of biological models, for example, the food-chain mathematical models, host–parasite theoretical prototypes, and laboratory experiments.[69–72]

In nonlinear dynamics, the equation

$$\beta = \frac{ds}{d\tau} = \Phi(s;m) = m - s^2 \tag{51}$$

represents the mathematical model of saddle-node bifurcations.[4,7] One may realize that $\Phi(s;m) = 0$ when $s^* = \pm\sqrt{m}$, where s^* is the equilibrium state of the order parameter. Here, we must emphasize that s^* is not a constant, as it shows dependence on the control parameter m. Figure 1(a) shows the saddle-node bifurcation diagram. From Eq. (51), we infer that $s^* = 0$ is the bifurcation point in the limit of $m \to m_C = 0$. From the CBT,[5,7,68,73] we may also conclude that the equilibrium state s^* can be stable or unstable depending on the value of the control parameter, as shown in Fig. 1(a).

Nevertheless, this conventional stability interpretation, which arises from the CBT, presents limitations since it is only local. For a critical equilibrium state, we could extract possible conclusions on the stability of the system if we could prove the existence of the Lyapunov functions for Eq. (51). However, the construction of these functions is an arduous task and imposes practical difficulties.[31,52] Hence, in order to obtain a complete characterization, one would be asked to supplement this local analysis through approximate techniques or numerical simulations.

Nonetheless, we shall show that it is possible to obtain global and local properties of the mathematical model right above by employing our formulation of information geometry. By Eqs. (30)–(34) and (51), we have

$$d\ell^2 = 8m(ds)^2 + 2(dm)^2, \tag{52}$$

which describes an invariant positive definite metric. As discussed earlier, we should note that the metric above is defined with respect to the reference equilibrium state s^*. Therefore, we must recognize that the metric elements $G_{\alpha\mu}$ are evaluated in the state $s = s^*$.

In order for the system, Eq. (51), to exhibit global stability in the structural sense, the necessary and sufficient conditions of the Sylvester criterion, Eq. (37), are

$$\begin{aligned} \Delta_1 &= 8m > 0, \\ \Delta_2 &= \begin{vmatrix} 8m & 0 \\ 0 & 2 \end{vmatrix} > 0. \end{aligned} \tag{53}$$

We must observe that m should be positive because $m < 0$ would lead to imaginary equilibrium values, otherwise. Therefore, one may conclude that Δ_1 and Δ_2 are never negative in the physical regime. Hence, we may write that our system is globally stable without the necessity of complicated global techniques or even numerical calculations.

Having discussed the global stability analysis, we now turn to local structural stability analysis through the interpretation of the curvature R. By Eq. (35), we have

$$\mathrm{R} = -\frac{1}{4m^2}. \tag{54}$$

The Fisher metric gives us an expression for R as a function of the derivatives of $\Phi(s;m)$. We now focus on the analysis of the graph and the sign of R. In Fig. 1(b), one can readily see that R is a negative function. Furthermore, it is a symmetric function of m. Therefore, R is independent of the orientation of m, i.e., $\mathrm{R}(-m) = \mathrm{R}(m)$. The graph of R has no m intercepts. We should note that $m^2 = 0$ when the system approaches the bifurcation point. As a consequence of that, the R-axis is the only vertical asymptote. On account of the fact

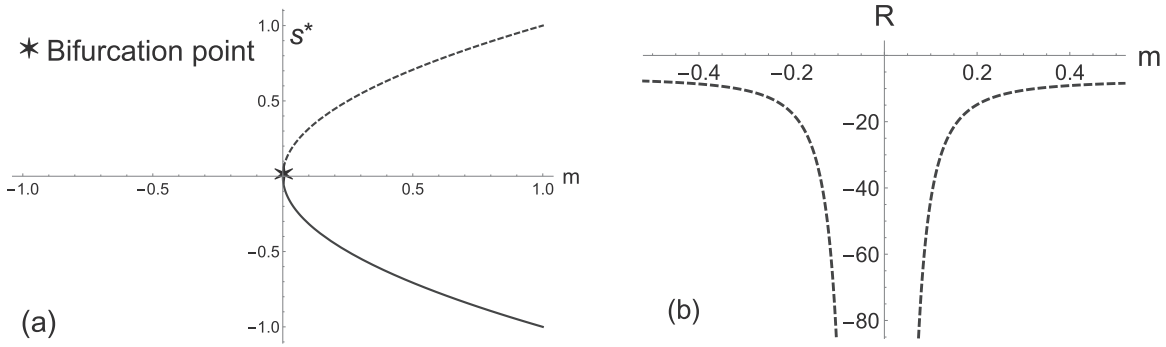

FIG. 1. (a) Shows the saddle-node bifurcation diagram, in which it is possible to observe the dependence of s^* on m. From the CBT, solid lines represent stability (Weinberg's sign convention assumed). Dashed lines refer to instability. We note that $s^* = 0$ describes the bifurcation point in the limit of $m \to m_C = 0$. (b) shows R as a function of m. In (b), the dashed line represents structural instability. As one may see, the curvature R is a real and a negative function of m everywhere in the real domain. So, $\mathrm{R}(-m) = \mathrm{R}(m)$. As a consequence of that, the function is even and the graph has R-axis symmetry. R is independent of the orientation of m. Here, R is interpreted as a measure of the local structural stability of the system under study. We may observe that R diverges as m^{-2} for $m > m_C$. In addition, we note that $\lim_{m\to 0^-} \mathrm{R} = -\infty$ and $\lim_{m\to 0^+} \mathrm{R} = -\infty$ for the system approaching m_C. Consequently, the R-diagram indicates that if R is large, then the system is less locally structural stable.

that the degree of the denominator is greater than the degree of the numerator, the m-axis is the horizontal asymptote.

Another remark concerns the local stability interpretation and the divergence of R. First, R is uniformly negative and decreases throughout the domain. Hence, we may write that the system is locally structural unstable. One may see from Fig. 1(b) that $R \to -\infty$ in the neighborhood of (s_C^*, m_C), that is to say, the singular point of R is coincident with the singularity of the dynamical system of Eq. (51). Here, the singularity appears at the bifurcation point. So, we may conclude that the system has a phase transition of type I. This latter is an important result since it teaches us that saddle-node bifurcations represent smooth transitions in the parameter space.

The interpretations derived above are in good agreement with the standpoint of view of previous works.[16,17,65,66]

B. Transcritical bifurcation

In general, transcritical bifurcations mark standard mathematical models with the exchange of stability in nonlinear sciences.[7,73] There are vast applications of the concept of transcritical bifurcations, e.g., lasers, population dynamics, and many others.[5,7,31] As a worked example, the equation

$$\beta = \frac{ds}{d\tau} = \Phi(s;m) = ms - s^2, \tag{55}$$

describes the normal form of transcritical bifurcations, in which $\Phi(s;m) = 0$, when $s_0^* = 0$ and $s_1^* \equiv s^* = m$. From the CBT,[5,7,68,73] we may conclude that s_0^* is unstable when $m < 0$. Alternatively, s_0^* becomes stable when $m > 0$ (sign convention assumed).

Conversely, s^* is unstable for $m > 0$. On the other hand, s^* becomes stable for $m > 0$. Furthermore, we may note that $s^* = 0$ in the limit of $m \to m_C = 0$. This denotes the bifurcation point. Figure 2(a) shows the behavior of the transcritical bifurcation. As one may observe, there is a remarkable exchange of stability nearby the critical region.

Nevertheless, the stability interpretation outlined above is, in some respect, incomplete because it is essentially a local analysis. With our aim of deriving a complete characterization of the system, we now turn to our approach to investigate bifurcations from the standpoint of information geometry.

One should note that Eq. (55) has two different equilibrium states. Therefore, we must perform separate analyses. For this purpose, we first dedicate ourselves to s^* and then we explore s_0^*.

According to the general rules developed in Sec. II, we obtain

$$d\ell^2 = 2m^2(ds)^2 + 2m^2(dm)^2, \tag{56}$$

in which the components of the metric tensor are evaluated in the state $s = s^*$.

The necessary and sufficient conditions of the Sylvester criterion are

$$\begin{aligned} \Delta_1 &= G_{11} > 0, \\ \Delta_2 &= \begin{vmatrix} G_{11} & 0 \\ 0 & G_{22} \end{vmatrix} > 0. \end{aligned} \tag{57}$$

Direct calculation shows

$$\Delta_1 = 2m^2, \quad \Delta_2 = 4m^4. \tag{58}$$

Despite the character of the control parameter m, we see that Δ_1 and Δ_2 are never negative in the physical regime. Consequently, one may conclude that our system presents global stability in the structural sense.

Having discussed the global analysis, we now dedicate ourselves to the local geometric analysis through the curvature R. By Eq. (35),

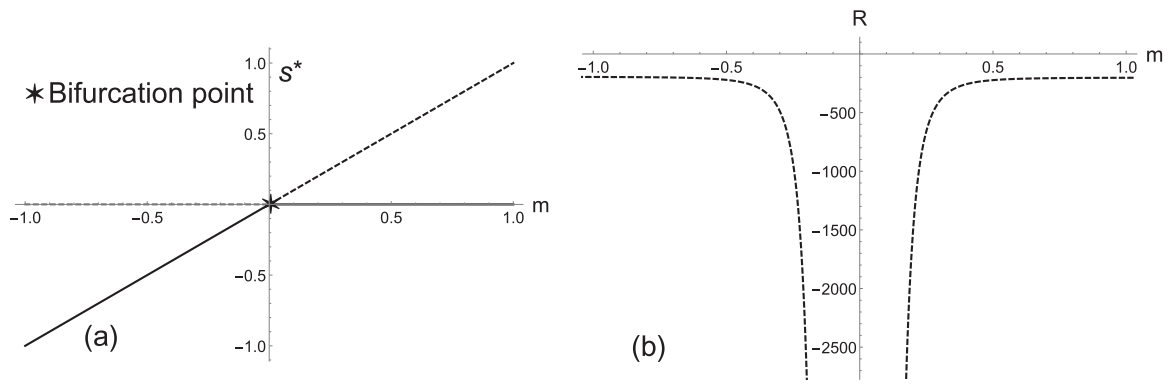

FIG. 2. (a) Shows the diagram of the transcritical bifurcation of Eq. (55). In addition, (a) qualitatively depicts the dependence of the equilibrium state on the control parameter m. Solid lines represent stability, while dashed lines refer to instability (Weinberg's sign convention assumed). We note that $s^* = 0$ in limit of $m \to m_C = 0$. This is the bifurcation point, in which there is a remarkable exchange of stability. On the other hand, (b) shows R as a function of m. Here, dashed lines represent structural instability. One can readily see that R is a negative symmetric function of m. The graph has no m intercepts. Here, $m^4 = 0$, when $m \to m_C$. As a consequence of this fact, we conclude that the R-axis is the only vertical asymptote. We may observe that the degree of the denominator is greater than the degree of the numerator. Hence, the m-axis is the horizontal asymptote. One may note that $\lim_{m\to 0^-} R = -\infty$ and $\lim_{m\to 0^+} R = -\infty$ when the system approaches m_C. Thus, the divergence of R marks the occurrence of transcritical bifurcations nearby the critical region. R is a measure of stability. Since R diverges as m^{-4} for $m > m_C$, then one can conclude that the system is locally structural unstable.

we find

$$\mathrm{R} = -\frac{1}{m^4}. \tag{59}$$

From the Fisher metric, we receive an expression for R as a function of the derivatives of $\Phi(s;m)$. We now focus on the graph and sign of R. Figure 2(b) shows the behavior of R on m. Analogously to the saddle-node bifurcation, we observe that $\mathrm{R}(-m) = \mathrm{R}(m)$. That is to say, R is independent of the orientation of m. We may also note that the R function is even. In addition, the graph of the curvature has R-axis symmetry. Another remark concerns the local structural stability and the divergence of R. First, the curvature scalar is uniformly negative and decreases throughout the domain. So, we may write that the system is locally structural unstable. This result agrees with the viewpoint of the previous works.[16,17,65,66] Second, we can see that the singular point of R is coincident with the singularity of the dynamical system, Eq. (55), as shown in Fig. 2(b). In the light of the foregoing, we may then conclude that the system has a transition of type I, i.e., a second-order phase transition.

We close this section by investigating the stability in the neighborhood of the equilibrium state s_0^*. In this state, Eq. (34) yields

$$d\ell^2 = G_{11}(ds)^2 + G_{22}(dm)^2, \tag{60}$$

where

$$G_{11} = 2\left(\frac{\partial\Phi(s;m)}{\partial s}\right)^2_{(s_0^*,\mathbf{m})} = 2m^2, \tag{61}$$

$$G_{22} = 2\left(\frac{\partial\Phi(s;m)}{\partial m}\right)^2_{(s_0^*,\mathbf{m})} = 0. \tag{62}$$

Nevertheless, it is not difficult to realize that the metric of Eq. (60) degenerates. This enables us to conclude that the trivial solution s_0^* is a purely mathematical equilibrium state without a necessarily physical interpretation. So, we cannot address stability considerations for s_0^* from our approach.

C. Pitchfork bifurcations

The normal form of pitchfork bifurcations, sometimes called forward, marks a broad range of symmetry-breaking models in nonlinear sciences. Applications of this bifurcation include, for example, sports,[74] statistical magnetic models,[75,76] neural oscillations,[77,78] and others.[30,31,79] The equation

$$\beta = \frac{ds}{d\tau} = \Phi(s;m) = ms - \gamma s^3, \tag{63}$$

represents the mathematical models of pitchfork bifurcations. However, we should recognize that Eq. (63) encompasses two contrasting bifurcations cases: supercritical, when $\gamma = 1$, and subcritical, when $\gamma = -1$. From Eq. (63), we realize that $s^* = \pm(m/\gamma)^{1/2}$ is the nontrivial equilibrium state of the order parameter. From the CBT[5,7,68,73] and Weinberg's sign convention, one may conclude that the equilibrium state s^* is locally unstable in the supercritical case. On the other hand, s^* is locally stable in the subcritical case ($\gamma = -1$).

We should recognize, further, that $s^* = 0$ in the limit of $m \to m_C = 0$. This denotes the bifurcation point. Figure 3 shows the behavior of pitchfork bifurcations in both configurations. In Fig. 3, we may observe a remarkable symmetry-breaking in the neighborhood of the critical regime.

Having discussed the conventional bifurcation analysis, we now seek to investigate pitchfork bifurcations from the standpoint of our formulation. By Eqs. (30)–(34) and (63), we have

$$d\ell^2 = 8m^2(ds)^2 + \frac{2m}{\gamma}(dm)^2, \tag{64}$$

which describes an invariant positive definite metric. Furthermore, we should note that the components of the metric tensor are evaluated in the state $s = s^*$.

Global stability requires

$$\Delta_1 = G_{11} > 0,$$
$$\Delta_2 = \begin{vmatrix} G_{11} & 0 \\ 0 & G_{22} \end{vmatrix} > 0. \tag{65}$$

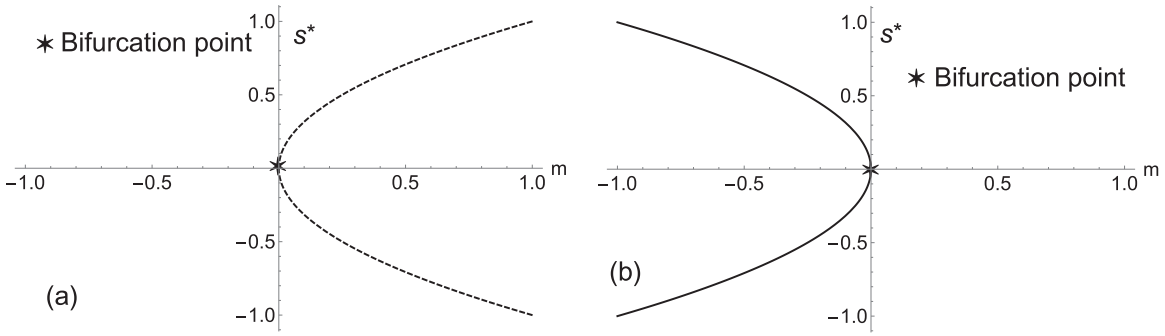

FIG. 3. It presents two contrasting diagrams of pitchfork bifurcations. (a) depicts the behavior of the supercritical pitchfork bifurcation ($\gamma = 1$), while the subcritical pitchfork ($\gamma = -1$) is shown in (b). The bifurcation diagrams also qualitatively show the dependence of the equilibrium state on the control parameter m. From the CBT, solid lines represent stability, while dashed lines refer to instability (sign convention assumed). We may note for both cases that if $m \to m_C = 0$, then $s^* = 0$, which marks the intriguing symmetry-breaking phenomena.

Direct calculation shows

$$\Delta_1 = 8m^2, \quad \Delta_2 = \frac{16m^3}{\gamma}. \tag{66}$$

Based on the above, it is not difficult to see that Δ_1 is always positive in the physical regime. However, we must recognize that the determinant Δ_2 may have different regimes due to the control parameter. Also important is the dependence of Δ_2 on the factor γ. Thus, we need interpret both cases separately. In the supercritical configuration ($\gamma = 1$), one can readily see that Δ_2 is positive in the region $0 < m < +\infty$. Consequently, we may conclude that there is a physical regime in which Δ_1 and Δ_2 are indeed positive. This reveals that the system may exhibit global stability in the structural sense.

In the subcritical configuration ($\gamma = -1$), however, we conclude that the system has both Δ_1 and Δ_2 positive and global stability in the region $-\infty < m < 0$.

Having discussed the conditions to assure global stability in the structural sense, we now study the divergence and local stability of the curvature R. By Eq. (35), we have

$$\mathrm{R} = -\frac{\gamma}{2m^3}. \tag{67}$$

Owing to the fact that the curvature scalar R has been determined, we shall investigate its dependence on the control parameter.

The R-diagrams of pitchfork bifurcations are plotted in Fig. 4. Figure 4(a) shows the stability behavior for supercritical bifurcation ($\gamma = 1$). Here, we may observe that $\mathrm{R} > 0$ when $m < 0$. In the region $-\infty < m < 0$, the R function is positive (stable). So, we can conclude that there is a gain of stability when the system approaches the critical point (s_C^*, m_C).

Conversely, one can readily see that $\mathrm{R} < 0$ when $m > 0$. Hence, R is negative (unstable) in the region $0 < m < +\infty$. This indicates that the system losses structural stability in the neighborhood of the critical point (s_C^*, m_C). We must also remark that there is a discontinuity in R for $m > m_C$. This reflects a first-order phase transition.[41,65,80] Furthermore, such discontinuity disappears at $m = m_C = 0$, that is, in the region $-\infty < m < 0$, where R is the positive (stable). Consequently, this denotes a second-order phase transition.

The behavior discussed in Fig. 4(a) teaches us that the critical point (s_C^*, m_C) occurs at a second-order transition that terminates a line of first-order transition. In statistical mechanics, the same behavior is also present in the Curie point of magnets and in the termination of the vapor–liquid transition in fluid systems.[41,81]

Having discussed the supercritical case, we now turn our attention to the behavior of R for the subcritical pitchfork bifurcation ($\gamma = -1$). Figure 4(b) depicts the dependence of R on the control parameter m. Here, we may observe that there is a discontinuity in R for $m < m_C$. Consequently, the R function is negative in the region $-\infty < m < 0$ (unstable). This result reflects a first-order phase transition. However, the discontinuity disappears in the region $0 < m < +\infty$ (stable), in which R is positive (stable). This indicates a second-order phase transition.[41,65,80]

Therefore, the analysis of the curvature scalar in Fig. 4 reveals that pitchfork bifurcations present signatures of two different types of phase transitions. The first one occurs when the curvature scalar diverges and shows changes in the sign of R, which denotes a phase transition of type I. The second one is due to the divergence of R when the system approaches the critical point, which indicates a phase transition of type II.

The observations obtained through the R-diagrams for the pitchfork bifurcations agree with the results of nonlinear studies. The conclusions here expand the state of the art since one usually does not see a pitchfork bifurcation as a second-order phase transitions with instances of first-order transitions.[74,82–84] We must remark that we have neglected the investigation of the trivial solution $s_0^* = 0$ in the analysis of pitchfork bifurcation. Analogously to the result found for transcritical bifurcation, the trivial solution of pitchfork

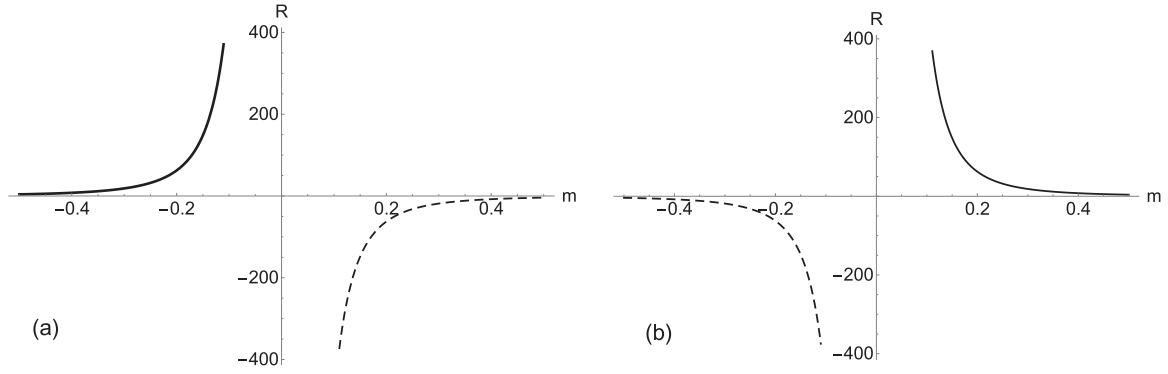

FIG. 4. (a) It depicts the dependence of R on m for the supercritical pitchfork bifurcation ($\gamma = 1$). We must remark that solid lines represent local structural stability, while dashed lines refer to local structural instability in the R-diagrams (Weinberg's sign convention assumed). The curvature R shows two different phase transitions. In the region $-\infty < m < 0$, R function is positive (stable), which reflects a phase transition of second order. In the region $0 < m < +\infty$, R is negative (unstable). Consequently, we conclude that there is a loss of structural stability when the system approaches the critical point. This produces a first-order phase transition. (b) shows R for the subcritical pitchfork bifurcation ($\gamma = -1$). In contrast to (a), $\mathrm{R} > 0$ when $m > 0$ and $\mathrm{R} < 0$ when $m < 0$. Here, we may observe that there is a discontinuity in R for $m < m_C$. In other words, R is negative (unstable) in the region $-\infty < m < 0$. This reflects a phase transition of first order. Nevertheless, the discontinuity disappears in the region $0 < m < +\infty$, in which R is positive (stable). This denotes a second-order phase transition. In both cases, we may observe that R is an odd function as it behaves differently from positive to negative values of m, i.e., $\mathrm{R}(-m) = -\mathrm{R}(m)$. One may also note that R diverges proportional to m^{-3}.

bifurcations also leads to a mathematical divergence of the metric. Hence, we cannot address physical interpretations for this case.

V. RESULTS II

In this section, we shall apply the results of our method to study the behavior, stability conditions, curvature R, and the character of the transitions of the homoclinic bifurcations present in the Duffing-like oscillator.

The procedure employed in this section is analogous to that considered earlier to study local bifurcations. Hence, we may organize this section as follows. First, we introduce the Duffing-like equation that consists of a modified version of the original equation of the Duffing oscillator. Second, we focus on stability conditions. Here, we first obtain the Fisher metric tensor by computing the derivatives of the nonlinear functions Φ_i. The global stability is analyzed through the Sylvester criterion. Our task here is to interpret the local square distance ($d\ell^2$) to verify whether or not the determinants Δ_i are positive definite. Finally, we interpret the diagrams of the curvature scalar with a special interest in its divergence.

A. The Duffing oscillator

The model upon which we shall base our considerations is that of Duffing's equation, which describes the dynamics of a curious oscillator composed of a metallic strip and AC electromagnets.[31,52,85] The model is to be considered as suggestive only, but it does lead to a qualitative understanding of the phenomena of homoclinic bifurcations.[52,86]

In nonlinear dynamics, the equations

$$\begin{cases} \beta_1 = \dfrac{ds_1}{d\tau} = \Phi_1(s_1, s_2) = s_2 \\ \beta_2 = \dfrac{ds_2}{d\tau} = \Phi_2(s_1, s_2) = s_1 - s_1^3 + \epsilon\left(m\, s_2 + s_1^2 s_2\right) \end{cases} \tag{68}$$

represent the modified mathematical model of the Duffing oscillator, where m is the control parameter and ϵ is a fixed perturbation parameter. Thus, we may write that the Duffing equation outlined above has only three varying parameters: s_1, s_2, and m. We should note that the present model presents a global homoclinic bifurcation when the perturbation ϵ of Eq. (68) is zero.[52,86] Homoclinic bifurcations,[87] however, cannot be detected by the CBT. Consequently, the study of this particular class of bifurcations is generally done through approximate methods, e.g., the harmonic balance, Melnikov's method, and numerical simulations.[52,88]

Nevertheless, we shall show that it is possible to study the phenomena of global bifurcations of the mathematical model right above by employing our formulation of information geometry. More specifically, the question that is posed here is whether or not information geometry might be employed to explore critical aspects of homoclinic bifurcations. By Eqs. (45)–(47) and (68), we have

$$d\ell^2 = 2\left(1 - 3s_1^2 + 2s_1 s_2\epsilon\right)^2 (ds_1)^2 + \left(2 + 2\epsilon^2\left(s_1^2 + m\right)^2\right)(ds_2)^2 + 2s_2^2\epsilon^2 (dm)^2,$$

which denotes an invariant positive definite metric. With our aim of investigating global bifurcations in mind, we cannot define the metric in the neighborhood of a reference state. Otherwise, the Riemannian metric would yield us a null curvature R.

For the present mathematical model, global stability requires

$$\Delta_1 = G_{11} > 0,$$
$$\Delta_2 = \begin{vmatrix} G_{11} & 0 \\ 0 & G_{22} \end{vmatrix} > 0, \tag{69}$$
$$\Delta_3 = \begin{vmatrix} G_{11} & 0 & 0 \\ 0 & G_{22} & 0 \\ 0 & 0 & G_{33} \end{vmatrix} > 0.$$

Direct calculation shows

$$\Delta_1 = 2\left(1 - 3s_1^2 + 2s_1 s_2\epsilon\right)^2, \tag{70}$$

$$\Delta_2 = \left(2 + 2\epsilon^2\left(s_1^2 + m\right)^2\right)\left(2\left(1 - 3s_1^2 + 2s_1 s_2\epsilon\right)^2\right), \tag{71}$$

$$\Delta_3 = \left(2s_2^2\epsilon^2\right)\left(2 + 2\epsilon^2\left(s_1^2 + m\right)^2\right) \tag{72}$$

$$\times \left(2\left(1 - 3s_1^2 + 2s_1 s_2\epsilon\right)^2\right), \tag{73}$$

whence we observe that Δ_1, Δ_2, and Δ_3 are never negative in the physical regime. Based on the above, we can write that the dynamical system, Eq. (68), satisfies the conditions of the Sylvester criterion. This allows us to conclude that the perturbed Duffing oscillator presents global stability in the structural sense.

However, it is important to recognize that the unperturbed Duffing equation violates the inequality of Eq. (72), since $\Delta_3 = 0$ for $\epsilon = 0$. This reveals an important finding in the understanding of homoclinic bifurcations in the framework of structural stability. The result found above enables us to conclude that the unperturbed oscillator does not present global stability. This is in agreement with Peixoto's theorem,[52,57] which establishes that homoclinic and heteroclinic bifurcations are both structurally unstable, based on the analysis of their phase portraits.

To conclude, we close this section by remarking that our geometric formulation shows an alternative approach to investigate instances of structural stability for global bifurcations without considering approximate methods or numerical solutions.

Having discussed the global analysis of stability in the structural sense, we now dedicate ourselves to the study of the curvature R. By Eqs. (48) and (49), we find

$$\mathrm{R} = \frac{\left(1-3s_1^2+2s_1s_2\epsilon\right)\left(1+s_1\left(4s_2\epsilon+s_1\left(-6+9s_1^2-12s_1s_2\epsilon+8s_2^2\epsilon^2\right)\right)\right)+2s_2\epsilon\left(1+\epsilon^2\left(s_1^2+m\right)^2\right)\left(s_1+9s_1^5-9s_1^4s_2\epsilon+s_1^3\left(-6+4s_2^2\epsilon^2\right)+s_2m\epsilon+s_1^2s_2\epsilon\left(5+\epsilon m\right)\right)}{\left(s_2^2\left(1-3s_1^2+2s_1s_2\epsilon\right)^3\left(1+\epsilon^2\left(s_1^2+m\right)^2\right)^2\right)}. \tag{74}$$

The Fisher metric leads us to an expression for the curvature scalar in terms of the derivatives of Φ_i. From the knowledge of R, we shall study its divergent behavior and the character of the transitions associated with the homoclinic bifurcations. Nevertheless, we must recognize that Eq. (68) behaves differently depending on the character of the perturbation ϵ. That is, the Duffing oscillator may assume two configurations: unperturbed, when $\epsilon = 0$; perturbed, when $\epsilon \geq 1$. Hence, we must interpret both cases separately.

Figure 5 depicts the behavior of R for the unperturbed configuration ($\epsilon = 0$). One can readily see that evaluations with Eq. (74) show that the curvature is uniformly positive and increases throughout the domain. Consequently, we infer that local structural stability is predominant in the physical regime.

Another remark concerning the behavior of the unperturbed oscillator is the divergence of R and its connection with bifurcations. As we have already proved, R diverges at singularities of dynamical systems, which appear at the bifurcation points.

In Fig. 5, one can readily see that R diverges in the neighborhood of the origin. To find the bifurcation point, the denominator of the curvature R should be zero. Therefore, it is not difficult to verify that R$\to \infty$, when

$$\left(s_2^2\left(1-3s_1^2+2s_1s_2\epsilon\right)^3\left(1+\epsilon^2\left(s_1^2+m\right)^2\right)^2\right)=0, \qquad (75)$$

in which it becomes evident that R diverges to positive infinity at the state $\left(s_1^*, s_2^*, m^*\right) = \left(\pm 1/\sqrt{3}, 0, -1/3\right)$. The procedure adopted above to find singular points of R is not a new idea here. This approach had already been considered to study critical aspects of the Kagome Ising model in the framework of thermodynamic geometry.[89]

However, we should emphasize that when $\epsilon = 0$, the dynamical system, Eq. (68), exhibits a homoclinic bifurcation in the phase portrait.[52,86] Consequently, this remarkable fact teach us that the divergence behavior of R marks the phenomenon of the homoclinic bifurcation, where $\left(s_1^*, s_2^*, m^*\right) = \left(\pm 1/\sqrt{3}, 0, -1/3\right)$ represents its bifurcation point.

In addition, this result shows that homoclinic bifurcations represent smooth transitions of type I in the parameter space when $\epsilon = 0$. The observations obtained through the R-diagrams for the homoclinic bifurcation agree very well with the results of nonlinear studies obtained through approximate global methods.[52,86] Furthermore, this shows a clear evidence in favor of the validity of our approach.

Having discussed the unperturbed configuration of the Duffing oscillator, we now dedicate ourselves to the study of the curvature R when the perturbation is large, that is to say, $\epsilon \geq 1$.

The R-diagram of the perturbed Duffing oscillator is plotted in Fig. 6, where we may observe that the curvature scalar is a negative function in the region $-\infty < s_1 < -1/3$. This indicates, locally, that the system loses structural stability in the neighborhood of the critical point. Conversely, in the region $-1/3 < s_1 < +\infty$, the curvature R is positive. Hence, we may infer that there is a gain of local structural stability in the physical regime.

One can readily see that R has a discontinuity in the neighborhood of the critical point $\left(s_1^*, s_2^*, m^*\right) = \left(\pm 1/\sqrt{3}, 0, -1/3\right)$. So, we may conclude that the R-diagram of the perturbed oscillator has a

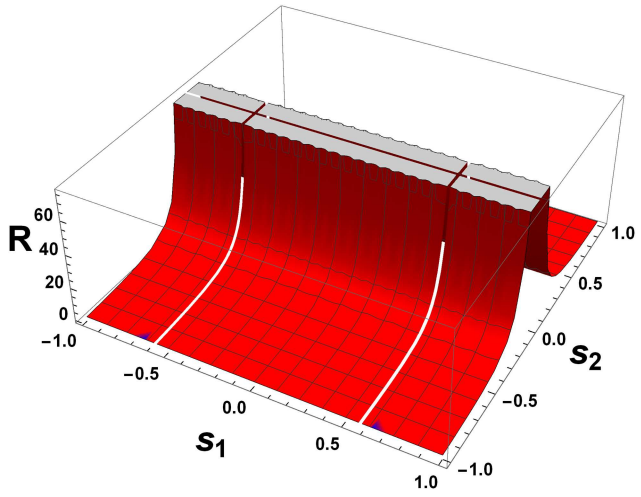

FIG. 5. It shows the behavior of the curvature R as a function of s_1 and s_2 for (s_1, s_2, m) variations in the unperturbed configuration of Duffing's oscillator ($\epsilon = 0$). One should note that the red color represents stability, while the blue color refers to instability. Evaluations with Eq. (74) show that R diverges at $\left(s_1^*, s_2^*, m^*\right) = \left(\pm 1/\sqrt{3}, 0, -1/3\right)$. R is real and positive in the physical regime. This enables us to conclude that Duffing's oscillator has a gain of local structural stability when the system approaches the critical point. Analogously to the saddle-node and transcritical cases, the system has a transition of type I.

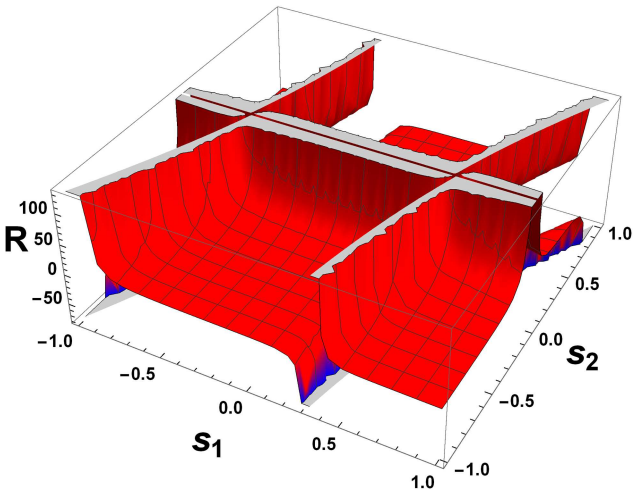

FIG. 6. It shows the behavior of the curvature R as a real function of s_1 and s_2 for (s_1, s_2, m) variations in the perturbed configuration of Duffing's oscillator. One should note that the red color represents stability, while the blue color refers to instability. For a sufficiently large perturbation ($\epsilon \geq 1$), evaluations with Eq. (74) show that the curvature is regular in the physical regime, except at $\left(s_1^*, s_2^*, m^*\right) = \left(\pm 1/\sqrt{3}, 0, -1/3\right)$, where the curvature R diverges. R is mostly positive, which we infer that local structural stability is predominant. The curvature R presents signatures of phase transitions of types I and II.

phase transition of type II that terminates at an isolated bifurcation point of a phase transition of type I. This particular type of phase transition has also been observed in the study of the critical phenomena of nuclear structures.[90]

Therefore, these analyses reveal two different types of phase transitions for homoclinic bifurcations. For the unperturbed configuration ($\epsilon = 0$), the Duffing oscillator presents a divergence of R. This denotes a phase transition of type I. On the other hand, for the perturbed configuration ($\epsilon \neq 0$), the curvature R changes its sign and diverges in the neighborhood of the state $(s_1^*, s_2^*, m^*) = (\pm 1/\sqrt{3}, 0, -1/3)$. This reflects a phase transition of type II.

To conclude, in the foregoing, we have, so far, extended our original geometric approach to investigate a non-trivial bifurcation in the context of the CBT. More precisely, we have studied the behavior, stability conditions, and the characterization of homoclinic bifurcations in a modified version of the Duffing oscillator.

VI. CONCLUSIONS

In this work, we aimed to overcome some of the limitations of the CBT by adding the geometric methods of information geometry. A general approach for local and global bifurcations is challenging. Consequently, the addition of information methods may be seen as a new hope when the standard bifurcation methods show little or no solution.

By following this premise, we have extended many features of the information geometry to investigate bifurcations in the context of dynamical systems. More precisely, we investigated the behavior, stability conditions, and the characterization of bifurcations through the interpretation of the Fisher metric and the curvature R.

In this article, a structural sense of global stability has been investigated for contrasting bifurcation models. In the study of the saddle-node and transcritical bifurcations, we have obtained positive definite metrics, which allowed us to conclude that both models are globally stable according to the Sylvester criterion. Nevertheless, in the investigation of pitchfork bifurcations, we have observed different conditions of global stability. In the supercritical configuration, we concluded that the system of Eq. (63) presents global stability in the region $0 < m < +\infty$, since both the determinants Δ_1 and Δ_2 are positive in the physical regime. Alternatively, in the subcritical configuration, we inferred that the system has both Δ_1 and Δ_2 positive and global stability in the region $-\infty < m < 0$.

In our analyses, a point of interest was the interpretation of local structural stability through the study of the sign of R. The saddle-node and transcritical bifurcations have negative curvatures. Hence, this allows us to conclude that both bifurcations are locally structural unstable in the neighborhood of the bifurcation point.

Also important is the divergent behavior of R for the saddle-node and transcritical equations. From our analyses, we found that these bifurcations have critical point divergences, i.e., $R \to -\infty$ nearby the bifurcation point (s_C^*, m_C). This character of transition occurs when the singularities of the curvature R coincide with the singularities of the dynamical systems. As a consequence of that, we see that the saddle-node and transcritical bifurcations have a transition of type I.

Nonetheless, this is quite unlike for the pitchfork bifurcations. In the supercritical pitchfork, the curvature scalar is positive in the region $-\infty < m < 0$. Furthermore, R tends to plus infinity at the critical point. So, we may conclude that there is a gain of local structural stability. Conversely, in the region $0 < m < +\infty$, R is negative and tends to negative infinity. Thus, we infer that the systems lose structural stability in the neighborhood of the critical point.

In the subcritical pitchfork, we observed that $R > 0$ when $m > 0$, thus reflecting a gain of local structural stability. On the other hand, $R < 0$ when $m < 0$. Hence, we may write that the system loses local structural stability in the neighborhood of the critical point.

In addition, the analyses of the R-diagrams revealed signatures of two different phase transitions for pitchfork bifurcations. The first transition is observed in virtue of the divergence of R as the system approaches the critical point. This indicates a transition of type I. The second transition takes place due to the changes in the sign of R. Thus, this denotes a phase transition of type II or a first-order transition according to the Ehrenfest classification.

Finally, as a result of the generalization of our geometric method, homoclinic bifurcations could be investigated in the framework of information geometry.

Homoclinic bifurcations belong to the class of global bifurcations that cannot be investigated through the CBT. In general, the analysis of homoclinic bifurcations is performed through time-consuming numerical simulations or approximate global methods. On account of the fact that the CBT fails to give a complete description of homoclinic bifurcations and the standard nonlinear methods present limitations, our formulation showed itself as an alternative viewpoint to investigate this problem.

In the framework of information geometry, we have observed different conditions for global stability of the Duffing oscillator. In the perturbed configuration, we conclude that the system satisfies the necessary and sufficient conditions to assure global stability according to the Sylvester criterion. Nevertheless, the unperturbed Duffing equation violates the inequality of Eq. (72), since $\Delta_3 = 0$ for $\epsilon = 0$. Hence, we concluded that the unperturbed oscillator does not present global stability, which agrees with Peixoto's theorem. This result represents an important finding in the comprehension of homoclinic bifurcations because it shows that our geometric formulation gives an alternative way to address stability for global bifurcations.

Another point of interest is the interpretation of the divergent behavior of R. In the unperturbed configuration, the curvature R is uniformly positive and increases throughout the domain, in which $R \to +\infty$ at the bifurcation point $(s_1^*, s_2^*) = (\pm 1/\sqrt{3}, 0, -1/3)$. Therefore, this remarkable fact shows that the homoclinic bifurcations represent smooth transitions of type I in the parameter space, when $\epsilon \to 0$.

The analysis of the R-diagram for the perturbed oscillator showed signatures of two different types of phase transitions. The first one happens because of the divergence of R when the system approaches the critical point. This indicates a phase transition of type I. The second one becomes evident given the fact that R shows a divergent behavior and changes its sign in the neighborhood of the bifurcation point. This denotes a phase transition of type II.

A further remark concerning the perturbed Duffing oscillator relies on the critical point $(s_1^*, s_2^*) = (\pm 1/\sqrt{3}, 0)$ and its respective bifurcation value $m^* = m_{\text{homoclinic}} = -1/3$. In general, it is not

possible to analytically determine either the bifurcation points or the parameter values in which a homoclinic bifurcation occurs. In this scenario, bifurcation points might be estimated through the Melnikov method. Even though this method is a universal technique to study global bifurcations, its practical use still has fundamental and technical difficulties.[91] In addition, we should note that the Melnikov approach can only give a reasonable analysis of the global behavior when the perturbation is very small or close to zero. For large perturbations, however, this method may not help us to understand the global behaviors of nonlinear systems.[91,92]

Based on the above, it becomes evident that our formulation expands the state of the art because the geometric methods derived here allowed us to analytically locate the bifurcation point and the parameter value of homoclinic bifurcations.

Nevertheless, we may recognize that the Riemannian metrical structure of the parameter space has some peculiarities for two-dimensional systems. We stress some of them here.

First, the derivation of the curvature R becomes a challenging task as the computation of the Christoffel symbols, the fourth-rank curvature tensor, and the curvature scalar R is not straightforward.

Second, if we consider two or one of s_1, s_2, or m to vary slowly compared with the others, thereby we may regard one of these as fixed, then the Fisher geometry might be investigated. Nonetheless, this possibility would allow us to analyze a particular system in seven different cases with one, two, or three independent parameters. The study of Riemannian metrics in an above-outlined manner is not a new idea here. This has already been considered to investigate stability and fluctuations in black holes thermodynamics.[15]

In the light of the foregoing, we may then write that we have successfully extended the geometrical methods of the information theory to investigate bifurcations in the framework of nonlinear dynamics. As a result, we have added a new theoretical possibility that allowed us to expand the state of the art of five contrasting bifurcation models. Also, the results obtained here agree precisely with those obtained some time ago by other methods and in somewhat different contexts.

In conclusion, we may write that our approach presents a clear improvement over the original CBT in essentially four ways. First, our formulation addresses global and local stability conditions for dynamical systems described by differential equations. Second, it encompasses the essential features of CBT. Third, global bifurcations may be investigated without considering approximate methods or numerical simulations. Finally, information geometry is a new approach not commonly used in nonlinear dynamics. As a natural corollary, our formulation provides an alternative way to study problems where the conventional nonlinear methods may show limitations. The physics presented in this article is, in most part, well understood, and it is a matter of the application of the techniques presented here to somewhat novel circumstances in the context of complex systems.

There are, of course, a few questions that remain open. First, the connection of the present formulation with the modern theory of critical phenomena, in which it is possible to assign critical exponents through standard assumptions on generalized homogeneous functions. Second, the application of the present geometric methods to study limit cycles and Hopf bifurcations. The details of the present theory on the Hopf bifurcations, limit cycles, and other global bifurcations will be postponed to the next articles of this series.

ACKNOWLEDGMENTS

V.B.d.S. is indebted to Professor H. Cabezas for helpful correspondence on the new trends and developments of the Fisher information theory. E.D.L. acknowledges support from CNPq (No. 301318/2019-0) and FAPESP (No. 2019/14038-6), Brazilian agencies. This work was supported by CAPES—Coordination for the Improvement of Higher Education Personnel. In addition, the authors wish to express their indebtedness to the anonymous reviewers for directing our attention to questions that have doubtlessly improved the original manuscript.

AUTHOR DECLARATIONS

Conflict of Interest

The authors have no conflicts to disclose.

DATA AVAILABILITY

Data sharing is not applicable to this article as no new data were created or analyzed in this study.

REFERENCES

[1] A. Collet, J. Bragard, and P. C. Dauby, "Temperature, geometry, and bifurcations in the numerical modeling of the cardiac mechano-electric feedback," Chaos **27**, 093924 (2017).
[2] L. Horwitz, Y. B. Zion, M. Lewkowicz, M. Schiffer, and J. Levitan, "Geometry of hamiltonian chaos," Phys. Rev. Lett. **98**, 234301 (2007).
[3] A. Mihara, "Thermodynamic geometry and critical aspects of bifurcations," Phys. Rev. E **94**, 012144 (2016).
[4] V. Afrajmovich, Y. Il'yashenko, L. Shil'nikov, V. Arnold, and N. Kazarinoff, *Dynamical Systems V: Bifurcation Theory and Catastrophe Theory* (Springer, 2013).
[5] H. Kielhöfer, *Bifurcation Theory: An Introduction with Applications to Partial Differential Equations* (Springer-Verlag, 2012).
[6] A. Lesne and M. Lagües, *Scale Invariance: From Phase Transitions to Turbulence* (Springer, 2011).
[7] E. D. Leonel, *Scaling Laws in Dynamical Systems* (Springer, 2021).
[8] V. B. da Silva, J. P. Vieira, and E. D. Leonel, "Fisher information of the kuramoto model: A geometric reading on synchronization," Physica D **423**, 132926 (2021).
[9] T. Vetsov, "Information geometry on the space of equilibrium states of black holes in higher derivative theories," Eur. Phys. J. C **79**, 71 (2019).
[10] K. Kolev, K. Staykov, and T. Vetsov, "Thermodynamic stability of the stationary lifshitz black hole of new massive gravity," Eur. Phys. J. C **79**, 1009 (2019).
[11] Z. M. Xu, W. L. Yang, and B. Wu, "Ruppeiner thermodynamic geometry for the schwarzschild-ads black hole," Phys. Rev. D **101**, 024018 (2020).
[12] G. Ruppeiner and A. Seftas, "Thermodynamic curvature of the binary van der waals fluid," Entropy **22**, 1208 (2020).
[13] G. Ruppeiner, "Thermodynamic curvature measures interactions," Am. J. Phys. **78**, 1170 (2010).
[14] G. Ruppeiner, "Stability and fluctuations in black hole thermodynamics," Phys. Rev. D **75**, 024037 (2007).
[15] G. Ruppeiner, "Thermodynamic curvature and phase transitions in Kerr–Newman black holes," Phys. Rev. D **78**, 024016 (2008).
[16] H. Janyszek and R. Mrugała, "Riemannian geometry and the thermodynamics of model magnetic systems," Phys. Rev. A **39**, 6515–6523 (1989).
[17] H. Janyszek and R. Mrugała, "Riemannian geometry and stability of ideal quantum gases," J. Phys. A: Math. Gen. **23**, 467 (1990).

[18]W. Janke, D. A. Johnston, and R. Kenna, "Information geometry and phase transitions," Physica A **336**, 181–186 (2004).
[19]N. H. Abdel-All, H. Abd-Ellah, and H. Mostafa, "Information geometry and statistical manifold," Chaos, Solitons Fractals **15**, 161–172 (2003).
[20]V. B. da Silva, "Statistical scaling laws for chemical oscillators," Physica A **509**, 66–73 (2018).
[21]D. Bakeš, L. Schreiberová, and I. Schreiber, "Mixed-mode oscillations in a homogeneous ph-oscillatory chemical reaction system," Chaos **18**, 015102 (2008).
[22]M. Iñarrea, J. F.Palacián, A. I. Pascual, and J. P. Salas, "Bifurcations of dividing surfaces in chemical reactions," J. Chem. Phys. **135**, 014110 (2011).
[23]I. T. Georgiou and F. Romeo, "Multi-physics dynamics of a mechanical oscillator coupled to an electro-magnetic circuit," Int. J. Non-Linear Mech. **70**, 153–164 (2015).
[24]L. Gardini, D. Fournier-Prunaret, and P. Chargé, "Border collision bifurcations in a two-dimensional piecewise smooth map from a simple switching circuit," Chaos **21**, 023106 (2011).
[25]V. B. da Silva and E. D. Leonel, "A scaling investigation for a van der pol circuit: Normal form applied to a hopf bifurcation," Int. J. Nonlinear Dynam. Control **1**, 154–170 (2018).
[26]V. B. da Silva, "Statistical scaling laws for competing biological species," Complex Syst. **27**, 355–368 (2018).
[27]H. Zhang, J. Kang, T. Huang, X. Cong, S. Ma, and H. Huang, "Hopf bifurcation, Hopf-Hopf bifurcation, and period-doubling bifurcation in a four-species food web," Math. Probl. Eng. **2018**, 8394651 (2018).
[28]R. E. Mirollo and S. H. Strogatz, "Synchronization of pulse-coupled biological oscillators," SIAM J. Appl. Math. **50**, 1645–1662 (2006).
[29]Y. Guo and A. C. J. Luo, "Parametric analysis of bifurcation and chaos in a periodically driven horizontal impact pair," Int. J. Bifurcation Chaos **22**, 1250268 (2012).
[30]A. J. Lichtenberg and M. A. Lieberman, *Regular and Chaotic Dynamics* (Springer-Verlag, 2013).
[31]S. H. Strogatz, *Nonlinear Dynamics and Chaos: With Applications to Physics, Biology, Chemistry, and Engineering* (CRC Press, 2014).
[32]M. M. Deza and E. Deza, *Encyclopedia of Distances* (Springer, 2013).
[33]M. K. Murray and J. W. Rice, *Differential Geometry and Statistics* (CRC Press, 1993).
[34]It should be emphasized here that s^* is not necessarily constant. In general, s^* may show dependence on the parameters of the dynamical systems.
[35]A. González-Mejía, L. Vance, T. Eason, and H. Cabezas, "Recent developments in the application of Fisher information to sustainable environmental management," in *Assessing and Measuring Environmental Impact and Sustainability*, 1st ed., edited by J. J. Kleme˘s (Butterworth-Heinemann, Oxford, 2015), Chap. 2, Vol. 1, pp. 25–72.
[36]V. Kampen, *Stochastic Processes in Physics and Chemistry* (Elsevier Science, 2007).
[37]T. Tomé and M. J. Oliveira, *Dinâmica Estocástica e Irreversibilidade*, 1st ed. (EDUSP, São Paulo, 2001), Acadâmica, Vol. 35.
[38]D. Bhatta and L. Debnath, *Integral Transforms and Their Applications* (CRC Press, 2016).
[39]It should be recognized that the Fourier transform can be defined by $\exp(J\kappa s)$ or either $\exp(-J\kappa s)$. These are essentially the same. However, here, we follow the well-known standard definition of the authors Kampen, Tomé, and Oliveira[36,37] to consider $g(\kappa)$ as the Fourier transform of the variable β.
[40]J. Schwinger and K. Milton, *Electromagnetic Radiation Variational Methods, Waveguides and Accelerators* (Springer, 2006).
[41]S. Salinas, *Introduction to Statistical Physics* (Springer, 2001).
[42]G. B. Arfken, F. E. Harris, and H. J. Weber, *Mathematical Methods for Physicists: A Comprehensive Guide* (Elsevier Science, 2013).
[43]E. Kreyszig, *Differential Geometry* (Dover Publications, 2013).
[44]G. Ruppeiner, "Thermodynamic curvature from the critical point to the triple point," Phys. Rev. E **86**, 021130 (2012).
[45]G. Ruppeiner, N. Dyjack, A. McAloon, and J. Stoops, "Solid-like features in dense vapors near the fluid critical point," J. Chem. Phys. **146**, 224501 (2017).
[46]The latter equation is achieved by employing the components of the metric tensor in the computation of the Christoffel symbols and, hence, the fourth-rank curvature tensor.[43]
[47]S. Weinberg, *Gravitation and Cosmology: Principles and Applications of the General Theory of Relativity* (Wiley & Sons, 1972).
[48]J. Rau, *Thermodynamics: An Introduction to Key Concepts* (Oxford University Press, 2017).
[49]H. Oshima, T. Obata, and H. Hara, "Riemann scalar curvature of ideal quantum gases obeying gentile's statistics," J. Phys. A: Math. Gen. **32**, 6373 (1999).
[50]It should be remarked here that we follow the standard Weinberg sign convention.[13,47]
[51]X. Liao and P. Yu, *Absolute Stability of Nonlinear Control* (Springer, Netherlands, 2008).
[52]L. H. A. Monteiro, *Sistemas Dinâmicos* (Livraria da Física, 2002).
[53]M. Thompson, J. M. T. Thompson, and H. B. Stewart, *Nonlinear Dynamics and Chaos* (Wiley, 2002).
[54]M. Hazewinkel, *Encyclopaedia of Mathematics* (Springer Netherlands, 2013), Vol. 6.
[55]C. Cichon, M. Radwanska, and Z. Waszczyszyn, *Stability of Structures by Finite Element Methods* (Elsevier Science, 2013).
[56]L. Meirovitch, *Computational Methods in Structural Dynamics* (Springer Netherlands, 1980).
[57]M. M. Peixoto, "Structural stability on two-dimensional manifolds," Topology **1**(2), 101–120 (1962).
[58]B. Dasgupta, *Applied Mathematical Methods* (Pearson Education, 2006).
[59]J. Pinele, S. I. R. Costa, and J. E. Strapasson, "On the Fisher-Rao information metric in the space of normal distributions," in *Geometric Science of Information*, 1st ed., edited by F. Nielsen and F. Barbaresco (Springer, Berlin, 2019), Vol. 11712, pp. 676–684.
[60]S. Hassani, *Mathematical Methods: For Students of Physics and Related Fields* (Springer, 2009).
[61]J. T. Katsikadelis, *Boundary Elements: Theory and Applications* (Elsevier Science, 2002).
[62]For simplicity, we are considering a dynamic system governed by differential equations, in which there is only a single control parameter. However, such consideration is not again a restriction but, rather, can be extended to dynamical systems with more than one single control parameter.
[63]Indeed, $R = 0$ does not teach us whether or not a system has bifurcations.
[64]Here, we once more have confined ourselves to the standard Weinberg sign convention, in which the negative sign of R is suppressed.
[65]S. Soroushfar, R. Saffari, and N. Kamvar, "Thermodynamic geometry of black holes in $f(R)$ gravity," Eur. Phys. J. C **76**, 476 (2016).
[66]F. Capela and G. Nardini, "Hairy black holes in massive gravity: Thermodynamics and phase structure," Phys. Rev. D **86**, 024030 (2012).
[67]T. Ma and S. Wang, *Phase Transition Dynamics* (Springer, 2019).
[68]G. C. Layek, *An Introduction to Dynamical Systems and Chaos* (Springer, 2015).
[69]J. Sardanyés, R. Martínez, and C. Simó, "Trans-heteroclinic bifurcation: A novel type of catastrophic shift," R. Soc. Open Sci. **5**, 129 (2018).
[70]K. McCann and P. Yodzis, "Biological conditions for chaos in a three-species food chain," Ecology **75**, 561–564 (1994).
[71]M. Groenenboom and P. Hogeweg, "Space and the persistence of male-killing endosymbionts in insect populations," Proc. R. Soc. Lond. B **269**, 2509–2518 (2002).
[72]L. Dai, D. Vorselen, K. Korolev, and J. Gore, "Generic indicators for loss of resilience before a tipping point leading to population collapse," Science **336**, 1175–1177 (2012).
[73]R. Seydel, *Practical Bifurcation and Stability Analysis* (Springer, 2010).
[74]C. Button, D. Araújo, K. Davids, N. B. Serre, and R. H. P. Passos, *Complex Systems in Sport* (Taylor & Francis, 2013).
[75]S.-Y. Kim, S.-H. Shin, J. Yi, and C. W. Jang, "Bifurcations in a parametrically forced magnetic pendulum," Phys. Rev. E **56**, 6613–6619 (1997).
[76]R. He and Q. Han, "Dynamics and stability of permanent-magnet synchronous motor," Math. Probl. Eng. **2017**, 8.
[77]A. Bose, "Bifurcations dynamics of single neurons and small networks," in *Encyclopedia of Computational Neuroscience*, 1st ed. (Springer, New York, NY, 2015).
[78]W. Jun-Jie, Z. Chun-rui, and L. Xiu-ling, "Bifurcation in two-dimensional neural network model with delay," Appl. Math. Mech. **26**, 210–217 (2005).

[79]J. Guckenheimer and P. Holmes, *Nonlinear Oscillations, Dynamcial Dynamics and Bifurcations* (Springer-Verlag, 2013).
[80]L. P. Kadanoff, *Statistical Physics: Statics, Dynamics and Renormalization* (World Scientific, 2000).
[81]D. A. Lavis and M. B. Bell, *Statistical Mechanics of Lattice Systems* (Springer-Verlag, 1999).
[82]C. Misbah, *Complex Dynamics and Morphogenesis: An Introduction to Nonlinear Science* (Springer Netherlands, 2016).
[83]J. Milton and T. Ohira, *Mathematics as a Laboratory Tool: Dynamics, Delays and Noise* (Springer, 2014).
[84]J. A. Freund and T. P;öschel, *Stochastic Processes in Physics, Chemistry, and Biology* (Springer, 2000).
[85]S. Celikovsky and I. Zelinka, "Chaos theory for evolutionary algorithms researchers," in *Evolutionary Algorithms and Chaotic Systems. Studies in Computational Intelligence*, 1st ed., edited by I. Zelinka, S. Celikovsky, H. Richter, and G. Chen (Springer, Berlin, 2010), Vol. 267, pp. 89–143.
[86]H. Sarmah, M. Das, T. Baishya, and R. Paul, "Homoclinic bifurcation in a second order differential equation," Int. J. Appl. Math. Stat. **5**, 29–40 (2016).
[87]Homoclinic bifurcations belong to the class of global bifurcations, in which a limit cycle collides with a saddle point. Global bifurcations are observed mainly when invariant structures collide with each other like invariant manifold and chaotic attractors, yielding to the destruction of the chaotic attractor. In this scenario, the destruction causes a considerable modification of the system's global topology, which cannot be studied by the CBT, i.e., local stability analysis, see Refs. 93–95.
[88]A. Ollero and F. Cuesta, *Intelligent Mobile Robot Navigation* (Springer, 2005).
[89]B. Mirza and Z. Talaei, "Thermodynamic geometry of a kagome ising model in a magnetic field," Phys. Lett. A **377**, 513–517 (2013).
[90]R. F. Casten, "Phase transional behavior in sherical-deformed transitions regions," in *Symmetries in Nuclear Structure*, 1st ed., edited by A. Vitturi and R. F. Casten (World Scientific, 2004), Vol. 1, pp. 172–181.
[91]Y. A. Tsarin, V. B. Ryabov, and D. M. Variv, "Problems of the application of Melnikov method for chaos forecast in Dissipative dynamical systems," in *Proceedings of the First International Conference on Unsolved Problems of Noise in Physics, Biology, Electronic Technology and Information Technology*, 1st ed., edited by C. R. Doering, L. B. Kiss, and M. F. Shlesinger (Hungary, 1996), Vol. 1, pp. 251–259.
[92]A. C. J. Luo, *Global Transversality, Resonance and Chaotic Dynamics* (World Scientific, 2008).
[93]G. F. Weber, *How Complexity Shapes the World* (Cambridge Scholars Publisher, 2021).
[94]E. D. Leonel, "Defining universality classes for three different local bifurcations," Commun. Nonlinear Sci. Numer. Simul. **39**, 520–528 (2016).
[95]L. Zhong, *Fuzzy Chaotic Systems: Modeling, Control, and Applications* (Physica-Verlag, 2006).